Detrital zircon provenance of north Gondwana Palaeozoic sandstones from Saudi Arabia

Guido Meinhold[1,2,*], Alexander Bassis[3,4], Matthias Hinderer[3], Anna Lewin[3] and Jasper Berndt[5]

[1]School of Geography, Geology and the Environment, Keele University, Keele, Staffordshire, ST5 5BG, UK;
[2]Abteilung Sedimentologie/Umweltgeologie, Geowissenschaftliches Zentrum Göttingen, Universität Göttingen, Goldschmidtstraße 3, 37077 Göttingen, Germany;
[3]Institut für Angewandte Geowissenschaften, Technische Universität Darmstadt, Schnittspahnstrasse 9, 64287 Darmstadt, Germany;
[4]Eurofins water&waste GmbH, Eumigweg 7, 2351 Wiener Neudorf, Austria and
[5]Institut für Mineralogie, Westfälische Wilhelms-Universität Münster, Corrensstraße 24, 48149 Münster, Germany

Author for correspondence: Guido Meinhold, Email: g.meinhold@keele.ac.uk

Abstract
We present the first comprehensive detrital zircon U–Pb age dataset from Palaeozoic sandstones of Saudi Arabia, which provides new insights into the erosion history of the East African Orogen and sediment recycling in northern Gondwana. Five main age populations are present in varying amounts in the zircon age spectra with age peaks at ~625 Ma, ~775 Ma, ~980 Ma, ~1840 Ma, and ~2480 Ma. Mainly igneous rocks of the Arabian–Nubian Shield are suggested to be the most prominent sources for the Ediacaran to middle Tonian zircon grains. Palaeoproterozoic and Archaean grains may be xenocrystic zircons or they have been recycled from older terrigenous sediment. A primary derivation from Palaeoproterozoic and Archaean basement is also possible, as rocks of such age occur in the vicinity. Approximately 4% of the detrital zircons show Palaeozoic (340–541 Ma) ages. These grains are likely derived from Palaeozoic post-orogenic and anorogenic igneous rocks of northeast Africa and Arabia. A few single grains gave up to Eoarchean (3.6–4.0 Ga) ages, which are the oldest zircons yet described from Arabia and its vicinity. Their origin, however, is yet unknown. Detrital zircons with U–Pb ages of ~1.0 Ga are present in varying amounts in all of the samples and are a feature of terrigenous sediment belonging to the Gondwana super-fan system with an East African–Arabian zircon province.

Keywords: U–Pb geochronology; sediment provenance; detrital zircon; Palaeozoic; north Gondwana; Saudi Arabia

1. Introduction

The Gondwana supercontinent formed by the closure of the Mozambique Ocean and subsequent amalgamation of East and West Gondwana during the Pan-African Orogeny at the end of the Neoproterozoic Era (e.g. Stern, 1994; Johnson *et al.* 2011). This led to the formation of a ~6000 km long accretionary orogen within Gondwana that extends from Arabia to East Africa and into Antarctica and is known as the East African Orogen (e.g. Stern, 1994; Johnson *et al.* 2011; Fritz *et al.* 2013), also referred to as the Transgondwanan supermountain (Squire *et al.* 2006). In NE Africa, the Pan-African Orogeny involved the collision of Archaean cratons and the Saharan Metacraton with the Arabian–Nubian Shield (Fig. 1a). The latter evolved between ~565 and 870 Ma and primarily comprises

Neoproterozoic juvenile oceanic island arcs (e.g. Stern, 1994; Johnson *et al.* 2011; Johnson, 2014).

After the assembly of Gondwana during the early Palaeozoic, a thick pile of quartz-rich sandstones was deposited across northern Gondwana (Fig. 1b), originally eroded from the Pan-African orogens (e.g. Garfunkel, 2002; Burke *et al.* 2003; Avigad *et al.* 2005; Meinhold *et al.* 2013). The high mineral maturity of the sediment can be attributed to either long transport distances and/or multi-stage sedimentary recycling (e.g. Garfunkel, 2002; Morag *et al.* 2011) or strong chemical weathering at the time of deposition (e.g. Avigad *et al.* 2005). The similarity of detrital zircon U–Pb age spectra in Palaeozoic sandstones throughout Gondwana let Squire *et al.* (2006) postulate the existence of large sediment fans that brought detritus from the East African Orogen towards the continental margins. Meinhold *et al.* (2013) extended the super-fan model to the northern Gondwana margin evaluating detrital zircon age spectra from Cambrian–Ordovician sandstones of North Africa, the Sinai Peninsula, and the northwesternmost part of the Arabian Peninsula. Stephan *et al.* (2019a) used a more extensive dataset, including also peri-Gondwana units, and evaluated the detrital zircon age spectra, using multivariate data analysis. Detrital zircon data from Lower Palaeozoic sedimentary rocks revealed three contrasting provenance end-members of the former Gondwanan shelf, namely the Avalonian, West African, and East African–Arabian zircon provinces (Stephan *et al.* 2019a,b). The East African–Arabian zircon province corresponds to the Gondwana super-fan system of Meinhold *et al.* (2013). Saudi Arabia would lie more distal along the sediment path to the northeast. However, the Gondwana super-fan model has not been tested yet for Saudi Arabia. Besides that, a thorough provenance analysis of detrital zircon ages from the Palaeozoic succession of Saudi Arabia does not yet exist.

In the present study, we analysed 24 sandstone samples from the Palaeozoic succession of Saudi Arabia (Fig. 2) to determine their detrital zircon U–Pb age spectra using laser ablation inductively coupled plasma mass spectrometry (LA–ICP–MS). The data are essential for refining the model of the Gondwana super-fan system of Meinhold *et al.* (2013) at a more distal location and thus for refining the East African–Arabian zircon province of Stephan *et al.* (2019a,b). In addition, they provide complementary provenance information for the Palaeozoic sandstones on the Arabian Peninsula. A more thorough understanding of the origin of these sedimentary units is important for reconstructions of palaeosource areas and sediment transport and gives novel insights into the erosion history of the East African Orogen. Besides that, the recognition of single zircon grains with up to Eoarchaean (3.6–4.0 Ga) ages in Palaeozoic sandstones of Saudi Arabia contributes further to the discussion whether hitherto unknown Early Archaean basement can be found in the Middle East (see Paquette & Le Pennec, 2012, 2013; Nutman *et al.* 2014) or whether such Early Archaean grains are rather recycled from old, distal sources.

2. Geological setting

In Saudi Arabia, the Palaeozoic succession crops out in a narrow band along the southern, eastern and northern margin of the Arabian Shield (Fig. 2a), which forms the eastern part of the Arabian–Nubian Shield (Fig. 1). The latter is a complex amalgamation of numerous intra-oceanic island arc terranes accreted between ~630 and 870 Ma, with igneous activity extending until ~565 Ma (Kröner, 1985; Stern, 1994; Johnson *et al.* 2011; Johnson, 2014). During the late Neoproterozoic, terrestrial sedimentary basins formed in which molasse was deposited under subaerial to shallow-water conditions, and variably interlayered with volcaniclastic rocks (Johnson *et al.* 2011, 2013). The Neoproterozoic rocks of the Arabian Shield are overlain with an erosional contact by Palaeozoic sandstones (Fig. 3a). Deposition took place from Cambrian to Permian times (Powers *et al.* 1966; Powers, 1968; Laboun,

2010) (Fig. 3a). Sedimentary environments varied, mainly ranging from fluvial braided stream setting to shallow marine, prodeltaic and open marine conditions (Dabbagh & Rogers, 1983; Stump & van der Eem, 1995; Al-Ajmi *et al.* 2015). The sediments were deposited on a stable continental shelf at a passive margin from the Cambrian until at least the Devonian (Stump & van der Eem, 1995; Sharland *et al.* 2001). The changes in accommodation space were primarily controlled by eustacy (Sharland *et al.* 2001). Low subsidence rates and the high stability of the Arabian Plate during most of the Palaeozoic resulted in a 'layer cake' stratigraphy (Bishop, 1995), although several erosional hiatuses and stratigraphic unconformities exist in the Palaeozoic succession (Stump & van der Eem, 1995). The erosional hiatuses separating sedimentary units are used for lithostratigraphic correlations (Stump & van der Eem, 1995; Laboun, 2010) (Fig. 3a). The Palaeozoic succession shows evidence for two Gondwana glaciations during the Late Ordovician (Hirnantian) (Clark-Lowes, 2005; Keller *et al.* 2011) and Carboniferous–Permian (McClure, 1980; Alsharhan *et al.* 1993; Keller *et al.* 2011). We refer to Keller *et al.* (2011), Al-Ajmi *et al.* (2015) and Bassis *et al.* (2016*a*) for details about sedimentary facies and depositional environment.

Siliciclastic sedimentary rocks, mainly quartz arenites, dominate the Lower Palaeozoic succession of Saudi Arabia (e.g. Fig. 3b; Bassis *et al.* 2016a). The dominance of the stable minerals, such as zircon, tourmaline and rutile (high ZTR index, as defined by Hubert, 1962), indicating sediment maturity, among the transparent heavy mineral assemblage characterizes the Lower Palaeozoic sandstones (Babalola, 1999; Hussain *et al.* 2004; Knox *et al.* 2007; Bassis *et al.* 2016*b*). Upper Palaeozoic sandstones are more feldspar rich (Fig. 3b) and contain unstable transparent heavy minerals like garnet and/or staurolite (e.g. Knox *et al.* 2007; Bassis *et al.* 2016*b*).

Whole-rock geochemistry and heavy mineral data reveal distinct changes in provenance between the Palaeozoic sandstones in central/northern (Tabuk area) and southern (Wajid area) Saudi Arabia (Bassis *et al.* 2016a,b) (Fig. 2a). Cambrian–Ordovician sandstones seem to be first-cycle sediments, probably sourced from the 'Pan-African' basement. The high mineralogical maturity of the sediment and the lack of apparent recycling trends seem to be a mixture of compositional variation of source rocks and reworking during deposition, coupled with intensive source area weathering and low sedimentation rates (see discussion in Bassis *et al.* 2016a). The overlying Upper Ordovician glaciogenic deposits likely consist of recycled Cambrian–Ordovician material. The Devonian–Permian sandstones show a significant influx of fresh basement material. The exact source for the Palaeozoic detritus is still under debate. The adjacent Arabian Shield most likely was a major contributor throughout the Palaeozoic, but far distant sources have to be taken into account as well (e.g. Al-Harbi & Khan 2008, 2011; Bassis *et al.* 2016b). Possible source areas to the south include Archaean to Palaeoproterozoic terranes in Yemen (e.g. Babalola, 1999; Hussain *et al.* 2004; Bassis *et al.* 2016*b*), metamorphic terranes in Eritrea and Sudan, as well as the Mozambique Belt in East Africa (Bassis *et al.* 2016b).

3. Methods

Samples analysed in this study were previously studied using thin-section petrography and whole-rock geochemistry (Bassis *et al.* 2016a) and conventional heavy mineral analysis including electron microprobe studies to determine the chemical composition of garnet and rutile grains (Bassis *et al.* 2016b). Samples were taken from surface outcrops in the Tabuk and Wajid study areas, respectively (Fig. 2). Lithology, stratigraphy and geographic coordinates of the studied samples are given in Table 1. After rock crushing, milling and dry sieving to obtain the 63–125 μm fractions, the heavy mineral fractions were separated using sodium polytungstate with a density of 2.85 g/mL (see Bassis *et al.* 2016*b* for details). Zircon selection from the heavy fractions was achieved by handpicking under a binocular microscope. Zircon grains were fixed in epoxy resin mounts and polished to expose the

interior of the grains. Prior to the analyses, transmitted light photomicrographs were taken with a polarizing microscope equipped with a camera system to study the zircon shape and roundness. Cathodoluminescence (CL) imaging was applied using a JEOL JXA 8900 RL electron probe microanalyzer (EPMA) equipped with a CL detector at the University of Göttingen (Department of Geochemistry, Geoscience Center) to reveal the internal structures (e.g. growth zones) and to guide spot placement in the zircon grains.

The U–Pb age determination was performed on a sector-field ICP–MS (Element2, ThermoFisher) coupled to a 193-nm Photon Machines Analyte G2 Excimer laser ablation system at the University of Münster (Institute of Mineralogy) following the procedure described in Lewin *et al.* (2020a). Isotope data were acquired on masses 202, 204, 206, 207 and 238. The mass 202 was used to quantify interference of ^{204}Hg on ^{204}Pb. A common Pb correction was only applied to an analysis if the fraction of common ^{206}Pb to total ^{206}Pb exceeded 1%. A summary of the laser ablation ICP–MS operation parameters is given in Table S1 in the Supplementary Material available online at https://doi.org/xxxxxxx.

Data reduction follows the procedure described by Kooijman *et al.* (2012). To account for the lower precision of ^{207}Pb/^{206}Pb values for young zircons, the data were filtered using two criteria as in previous detrital zircon provenance studies (Löwen *et al.* 2017; Lewin *et al.* 2020a): accepted were all zircon ages (1) with 90–110% concordance [100 × (^{206}Pb/^{238}U/^{207}Pb/^{235}U)] for grains younger than 1200 Ma, and (2) with 90–110% concordance [100 × (^{206}Pb/^{238}U /^{207}Pb/^{206}Pb)] for grains older than 1200 Ma. This age was chosen due to the natural gap of zircon ages in the analysed samples. The R-package Provenance (Vermeesch *et al.* 2016) was used for visualization of the zircon age spectra as kernel density estimates (KDE) and for multi-sample comparison using multidimensional scaling (MDS). MDS is a useful technique to interpret, for example, large detrital zircon U–Pb age datasets by statistically comparing the data and visualizing all in a simple two-dimensional map in which 'similar' samples plot close together and 'dissimilar' samples plot far apart (e.g. Vermeesch, 2013; Vermeesch & Garzanti, 2015). The international chronostratigraphic chart of Cohen *et al.* (2018) was used as a stratigraphic reference for data interpretation.

4. Results

From the 24 sandstone samples of the Palaeozoic succession of Saudi Arabia, in total, 1915 zircon ages have been obtained of which 1734 ages (91% of all zircons) are 90–110% concordant (Table 1) using the respective data filters described in Section 3. Complete data sets used here are reported in Table S2 in the Supplementary Material available online at https://doi.org/xxxxxxx.

The majority of the detrital zircons are clear or translucent. Subrounded to rounded grains are dominant. Most of the zircons show undisturbed oscillatory (magmatic) zoning in the CL images (Fig. 4). Many grains also show regrowth features suggesting that these grains have subsequently recrystallized during late- or post-magmatic cooling (Corfu *et al.* 2003). Zircons with xenocrystic cores and clearly zoned rims are minor.

Five main detrital zircon populations are identified in the Palaeozoic sandstones of the Wajid and Tabuk areas of Saudi Arabia with main age peaks at ~625 Ma, ~775 Ma, ~980 Ma, ~1840 Ma and ~2480 Ma (Fig. 5). Detrital zircons with Ediacaran–Cryogenian (541–720 Ma) ages are most prominent making up ~36% of all concordant dates. A minor amount of all concordant zircon grains, approximately 4% show Palaeozoic (340–541 Ma) and approximately 0.6% show up to Palaeo- and Eoarchaean (3200 to <4000 Ma) ages.

In the following, the zircon data are presented independently for both study areas starting for each with the oldest stratigraphic formation. We also mention the youngest zircon age for each sample/formation. However, we caution against overinterpretation of these ages in regard to estimation of the maximum age of deposition. A small amount of Pb loss can shift

the U–Pb zircon age along the concordia curve toward younger ages, but the age will remain concordant using the filtering criteria as outlined in Section 3. Nonetheless, Dickinson & Gehrels (2009) could exemplarily show for the Mesozoic sedimentary succession of the Colorado Plateau that the youngest single grain zircon ages are compatible with depositional age for >90% of the samples, and lie within 5 Ma of depositional age for ~60% of the samples. Also, the weighted arithmetic mean of the youngest population of detrital zircon ages is often used for the estimation of the maximum age of deposition (Dickinson & Gehrels, 2009). However, we did not apply that here as (1) not each sample provided the required minimum number ($n \geq 3$) of grains for the youngest zircon population that overlap in age at 2 standard deviations and (2) this approach does also have its shortcomings (see Spencer *et al.* 2016 for details).

4.a. Wajid area

Nine Palaeozoic sandstone samples from the Wajid area were analysed for their detrital zircon age spectra (Figs 2b, 6, 7; Table 1). In total, 704 zircon ages have been obtained of which 636 ages (90.3% of all zircons) are 90–110% concordant.

Dibsiyah Formation (Cambrian–Ordovician): Both samples show similar zircon age spectra. The majority of all grains yielded Ediacaran–Cryogenian (541 to <720 Ma; 49% and 44%, respectively) and Tonian (720 to <900 Ma; 33% and 25%, respectively) ages (Fig. 7). Sample 74 shows a higher amount of Tonian–Stenian (900–1200 Ma) ages than sample 79 (i.e. 12% versus 5%). This correlates with a higher amount of Ectasian–Siderian (1200 to <2500 Ma) zircon ages in sample 74 than in sample 79 (i.e. 10% versus 3%). Palaeozoic zircon grains are minor (5%) as are Archaean zircon grains (4%). The youngest zircon age in the Dibsiyah Formation is 481 ± 22 Ma (sample 79, analysis number, #: 56) whereas the oldest age is 3522 ± 38 Ma (sample 74, #: 30) (Fig. 4).

Sanamah Formation (Upper Ordovician): From two samples (73 and 62), in total, 164 zircon ages have been obtained of which 136 have been used for interpretation. Both samples show very similar zircon age spectra, with most grains yielding Ediacaran–Cryogenian (32% and 33%, respectively) and Tonian (32% and 33%, respectively) ages (Fig. 7). Sample 73 shows more Tonian–Stenian (900–1200 Ma) ages than sample 62 (i.e. 21% versus 13%). The amount of Ectasian–Siderian zircon ages is almost equal in both samples (i.e. 10% versus 8%). Palaeozoic zircon grains are minor (5% and 6% respectively). Sample 62 yielded more Archaean ages than sample 73 (6% and 1% respectively). The youngest zircon age in the Sanamah Formation is 453 ± 10 Ma (sample 73, #: 33). The oldest age is 2735 ± 21 Ma (sample 62, #: 3).

Khusayyayn Formation (Devonian): In total, 260 zircon ages from three samples (118, 90, and 87) of the have been obtained of which 244 have been used for interpretation. Samples 90 and 87 show similar zircon spectra with the majority of all grains yielding Ediacaran–Cryogenian (22% and 26%, respectively), Tonian–Stenian (34% and 32% respectively), and Ectasian–Siderian (25% and 18% respectively) ages (Fig. 7). The amount of Tonian (13% and 10%, respectively) ages is less compared with older Palaeozoic sandstone samples. Sample 118 shows a different zircon age spectrum given that it has more grains with Ediacaran–Cryogenian (34%) and Tonian (30%) ages (Fig. 7). Palaeozoic zircon grains make up less than 3%. The amount of Archaean zircon grains ranges from 4 to 9%. The youngest zircon age in the Khusayyayn Formation is 494 ± 22 Ma (sample 90, #: 11) whereas the oldest zircon age is 3347 ± 13 Ma (sample 87, #: 89).

Juwayl Formation (Carboniferous–Permian): From two samples (100 and 98), in total, 114 zircon ages have been obtained of which 106 have been used for interpretation. The low number of obtained ages is due to the low zircon fertility of sample 98. The majority of the zircons fall into the Ediacaran–Cryogenian (40% and 54%, respectively) and Tonian (24% and 21%, respectively) age groups (Fig. 7). The amount of Tonian–Stenian (900–1200 Ma)

ages is broadly similar in both samples (i.e. 12% versus 17%) whereas the amounts of Ectasian–Siderian ages are different (i.e. 18% versus 8%). Both the youngest (362 ± 8 Ma, #: 72) and oldest (2612 ± 23 Ma, #: 25) zircon ages in the Juwayl Formation come from sample 100.

4.b. Tabuk area

Fifteen Palaeozoic sandstone samples from the Tabuk area were analysed for their detrital zircon age spectra (Figs 2c, 6, 7; Table 1). In total, 1211 zircon ages have been obtained of which 1098 ages (90.7% of all zircons) are 90–110% concordant.

Saq Formation (Cambrian–Ordovician): From two samples (170 and 169), in total, 165 zircon ages have been obtained of which 141 have been used for interpretation. In both samples, Ediacaran–Cryogenian (42% and 33%, respectively), Tonian (26% and 15%, respectively), and Tonian–Stenian (14% and 31%, respectively) age groups are most prominent but in varying amounts (Fig. 7). Ectasian–Siderian (i.e. 12% versus 13%) and Archaean (i.e. 8% versus 9%) zircon ages are minor with almost equal amounts in both samples. The youngest (549 ± 11 Ma, #: 39) and oldest (2660 ± 20 Ma, #: 3) zircon ages in the Saq Formation come from sample 169.

Qasim Formation (Ordovician): In total, 299 zircon ages from four samples (144/1, 145, 126, and 124) have been obtained of which 259 have been used for interpretation. The oldest samples 144/1 and 145 show similar zircon spectra with the majority of all grains yielding Ediacaran–Cryogenian (47% and 43%, respectively) and Tonian (27% and 41% respectively) ages (Fig. 7). Tonian–Stenian (900–1200 Ma) ages are only minor (6% and 2% respectively). Ectasian–Siderian (14% and 8% respectively) and Archaean (4% and 2% respectively) ages are subordinate present in both samples. The youngest samples 126 and 124 show similar zircon spectra. Compared with the oldest samples, however, they show lower amounts of Ediacaran–Cryogenian (27% and 26%, respectively), slightly lower to almost equal amounts of Tonian (31% and 22% respectively) but higher amounts of Tonian–Stenian (19% and 16% respectively) and Ectasian–Siderian (19% and 21% respectively) ages (Fig. 7). There is an increase in the amount of Palaeozoic zircon grains with stratigraphy from old (1%) to young (9%) (Fig. 7). The youngest and oldest zircon ages in the Qasim Formation are 476 ± 10 Ma (sample 145, #: 14) and 2795 ± 16 Ma (sample 144/1, #: 73), respectively.

Sarah and Zarqa formations (Upper Ordovician): In total, 165 zircon ages were obtained, with 148 ages being 90–110% concordant. Sample 123/2, from the Sarah Formation, and sample 132/1, from the Zarqa Formation, show similar zircon age spectra with the majority of the ages falling into the Ediacaran–Cryogenian (45% and 37%, respectively) and Tonian (25% for each sample) age groups (Fig. 7). The amounts of Tonian–Stenian (9% and 11%, respectively) and Ectasian–Siderian (11% for each sample) zircon ages are almost equal in both samples. Archaean ages (1% and 3%, respectively) are almost absent. Interestingly, the increase in the amount of Palaeozoic zircon grains with stratigraphy from old (9% in sample 123/2) to young (13% in sample 132/1) seems to continue in the Upper Ordovician (Fig. 7). Sample 132/1 yielded both the youngest (466 ± 14 Ma, #: 36) and oldest (3066 ± 31 Ma, #: 30) zircon ages among the Upper Ordovician sample set.

Tawil, Jauf, and Jubah formations (Devonian): In total, 407 zircon ages from five samples (157, 156, 160/T, 152, and 150) have been obtained of which 384 have been used for interpretation. The oldest Devonian samples (157 and 156) are from the Tawil Formation, and they show different zircon spectra compared to the remaining Devonian samples. In both Tawil Formation samples, Ediacaran–Cryogenian (33% and 40%, respectively) ages are most prominent followed by Tonian (20% and 17% respectively) and Tonian–Stenian (29% and 19% respectively) zircon age groups (Fig. 7). The amount of zircon ages belonging to the Ectasian–Siderian (10% and 7% respectively) age group is almost similar in both samples. Archaean ages (8% and 12% respectively) are more prominent compared to samples from

Lower Palaeozoic formations. The remaining Devonian samples from the Jauf and Jubah formations show lower amounts of Ediacaran–Cryogenian (less than 23%) but higher amounts of Tonian (23–24%) and much higher amounts of Tonian–Stenian (33–38%) ages compared to the samples from the Tawil Formation (Fig. 7). The amounts of zircon ages belonging to the Ectasian–Siderian (7–11%) and Archaean (7–10%) age groups in the Jauf and Jubah formations is similar to those of the Tawil Formation samples (Fig. 7). The youngest zircon age in the Devonian samples is 439 ± 6 in sample 156 (#: 44). The Devonian samples yielded a high amount of Palaeo- and Eoarchean ages and surprisingly, the oldest zircon ages among the Palaeozoic samples from Saudi Arabia: 3771 ± 37 Ma (#: 82) and 3850 ± 25 Ma (#: 38) in the Jubah Formation sample 152 (Figs 4, 5).

Unayzah Formation (Carboniferous–Permian): From two samples (129 and 120), in total, 175 zircon ages have been obtained of which 166 have been used for interpretation. Both samples show similar zircon age spectra with the majority of the ages falling into the Ediacaran–Cryogenian (46% and 49%, respectively) and Tonian (19% and 25%, respectively) age groups (Fig. 7). Sample 120 has more Tonian–Stenian (900–1200 Ma) zircon ages than sample 129 (i.e. 14% versus 9%). The amount of Ectasian–Siderian ages is almost equal in both samples (i.e. 11% versus 10%). Palaeozoic (both samples 4%) and Archaean (7% and 4%, respectively) ages are minor present. Both the youngest (340 ± 8 Ma, #: 78) and oldest (3631 ± 24 Ma, #: 58) zircon ages in the Unayzah Formation come from sample 120.

5. Discussion

The first comprehensive detrital zircon age analysis of Palaeozoic sandstones from Saudi Arabia presented here revealed three prominent age populations at ~625 Ma, ~775 Ma, and ~980 Ma, accompanied by two minor age populations at ~1840 Ma and ~2480 Ma (Fig. 5). These age populations are similar to those identified by Garzanti *et al.* (2013) in two Palaeozoic sandstone samples from the Tabuk area. However, we do not further discuss these two samples due to their uncertain stratigraphic assignment. For example, Garzanti *et al.* (2013) described an Ordovician sandstone sample, which they assigned to the 'Tabuk Formation'. However, that term has been discarded long ago (see Laboun, 2010).

5.a. Possible source areas

As most of the zircons show oscillatory zoning and some showing regrowth features in the CL images (Fig. 4), igneous rocks are the primary source of these grains. The Ediacaran–Cryogenian (541 to <720 Ma) and the Tonian (720 to <900 Ma) age groups represent igneous events associated with the Pan-African Orogen. Igneous crustal domains in the Arabian–Nubian Shield and the Eastern Granulites–Cabo Delgado Nappe Complex in the Mozambique Belt are likely sources, in agreement with palaeocurrent data, as igneous rocks with ages between 541 and 900 Ma are well known from these areas (e.g. Kröner, 1985; Stern, 1994; Johnson *et al.* 2011; Fritz *et al.* 2013; Johnson, 2014). Although it is difficult to narrow down the exact source, the ~625 Ma zircon age peak in the studied samples (Fig. 5) is likely related to the youngest crustal growth phases in the Arabian–Nubian Shield, which are found in the eastern Arabian Shield and northern Nubian Shield. Also, ~628 Ma old plutonic rocks occur in the western Nubian Shield (e.g., granodiorite at Gebel el-Asr in southern Egypt: Zhang *et al.* 2019a) and 630–500 Ma igneous rocks are known from the southern Nubian Shield (e.g., granitoids in the Southern Ethiopian Shield: Teklay *et al.* 1998; Yibas *et al.* 2002; Stern *et al.* 2012). The ~775 Ma zircon age peak (Fig. 5) is likely related to the oldest crustal growth phases, which are found in the western Arabian Shield and the southern Nubian Shield (Fritz *et al.* 2013).

The few early Palaeozoic ages (439–541 Ma) reported in almost all of the samples (Fig. 7) could be derived from post-orogenic igneous rocks. Cambrian post-orogenic plutonic

rocks are known from the Arabian–Nubian Shield and southeast Africa and Madagascar (Fritz *et al.* 2013). Cambrian and Ordovician alkaline and peralkaline plutonic rocks occur in Egypt and Sudan (Höhndorf *et al.* 1994; Woolley, 2001; Veevers, 2007). In addition, early Palaeozoic post-orogenic plutonic rocks, volcanic rocks and related products, such as volcanic ash beds (K-bentonites), as described from the Middle Ordovician of Libya (Ramos *et al.* 2003), and ascribed to volcanic activity along the northern margin of Gondwana during that time, could be an additional or alternative source (Meinhold *et al.* 2011; Lewin *et al.* 2020a). Late Devonian–Early Carboniferous zircons may come from within-plate, anorogenic igneous rocks from localized regions of northeast Africa and Arabia, as known, for example, from Levant and its vicinity (e.g. Stern *et al.* 2014; Golan *et al*. 2018). The youngest zircon ages in the studied samples should not be overinterpreted, as they are commonly single ages. Similar to the detrital zircons from Ethiopia (Lewin *et al.* 2020a), some of the early Palaeozoic zircons from sandstones of Saudi Arabia were corrected for common Pb, and thus they may be over-corrected, leading to younger ages.

The pre-900 Ma zircon ages in the studied samples may have originally been xenocrystic zircons in Pan-African igneous rocks of the East African Orogen. This, however, will not be applicable to the majority of the pre-900 Ma ages recorded in the studied samples. Stern *et al.* (2010) have shown that only 5% of individually dated zircons from igneous rocks of the Arabian–Nubian Shield are older than 880 Ma, with prominent age populations at 0.9–1.15 Ga (Tonian–Stenian), 1.7–2.1 Ga (late Palaeoproterozoic), 2.4–2.8 Ga (Palaeoproterozoic–Neoarchaean), and 3.2–3.5 Ga (Palaeoarchaean). Furthermore, most of the zircons analysed here have oscillatory (magmatic) zoning in the CL images, with xenocrystic cores a very minor component. Therefore, other sources than 'xenocrystic' zircons need to be considered for the pre-900 Ma detrital zircons.

The nearest basement rocks with Tonian–Stenian (900 to <1200 Ma) ages are documented from Sudan and the Sinai Peninsula. Kröner *et al.* (1987) described high-grade metasedimentary gneisses at Sabaloka in Sudan containing detrital zircons ranging in age from 2.6 to 0.9 Ga. Küster *et al.* (2008) described ~900–920 Ma-old metamorphic zircons from basement rocks of the Bayuda terrane in Sudan, which indicate an orogenic event preceding the East African Orogeny. Both the Saboloka and Bayuda basement units belong to the eastern Saharan Metacraton (Fig. 1b). Be'eri-Shlevin *et al.* (2009) reported 0.9–1.13 Ga-old zircons from the Sa'al schist in Sinai. This, together with the euhedral shape of some of these grains and the lack of other pre-Neoproterozoic zircon ages in the Sa'al schist is taken as evidence for the presence of 0.9–1.1 Ga-old crust at the northeastern margin of western Gondwana prior to the formation of the Arabian–Nubian Shield (Be'eri-Shlevin *et al.* 2009). Such crust is preserved as calc-alkaline volcanic and intrusive rocks (1.02–1.03 Ga) within the Sa'al metamorphic complex on Sinai (Be'eri-Shlevin *et al.* 2012). Although the Sinai basement is in proximity to the study area, at least to the Tabuk area, sediment supply from the ~1 Ga basement seems unlikely, as palaeocurrent data point toward a southerly provenance (Dabbagh & Rogers, 1983; Stump & van der Eem, 1995; Babalola, 1999; Hussain *et al.* 2000). However, at least for the Wajid area, a prevailing northward transport direction cannot be inferred for the entire Palaeozoic succession, as opposing (NW to SE) transport directions occur in the glaciogenic units of the Upper Ordovician Sanamah Formation and the Carboniferous–Permian Juwayl Formation (Hinderer *et al.* 2009; Keller *et al.* 2011; Al-Ajmi *et al.* 2015). A change of the prevailing northward transport direction seems to have started during the Devonian because in the Wajid area, dip measurements of cross-bedding indicate palaeocurrent directions to the north and north-northeast in the lower Khusayyayn Formation and already more easterly directions in the upper Khusayyayn Formation (Stump & van der Eem, 1995). The Arabian–Nubian Shield including its northernmost part on the Sinai Peninsula could thus be a possible source area. However, minor amounts of ~1 Ga zircons are present in Neoproterozoic diamictites of northern Ethiopia (Avigad *et al.* 2007) and the

Eastern Desert of Egypt (Ali *et al.* 2010). Thus, some ~1 Ga zircons may have been recycled from Neoproterozoic siliciclastic sediments but this does probably not account for the majority of the ~1 Ga zircon grains in the studied Palaeozoic sandstones. The source of the ~1 Ga zircons will be further discussed in Section 5.c in regard to the Gondwana super-fan system and the East African–Arabian zircon province, respectively.

Palaeoproterozoic and Archaean detrital zircons recorded in Palaeozoic sandstones of Saudi Arabia may have been recycled from Neoproterozoic sediments of the Arabian–Nubian Shield, as these sediments contain Palaeoproterozoic and Neo- and Mesoarchaean detrital zircon grains (Agar *et al.* 1992; Wilde & Youssef 2002; Ali *et al.* 2010). Alternatively, they may represent xenocrystic cores originally derived from igneous rocks of the Arabian–Nubian Shield, but this would only account for a small number of grains (see Stern *et al.* 2010). A primary derivation from Palaeoproterozoic and Archaean basement is also likely, as meta-igneous rocks of such age occur in the vicinity of the study area, e.g. ~1.66 Ga crust (and probably also older crust based on Sm–Nd isotope data) in the Khida terrane of the eastern Arabian Shield (Whitehouse *et al.* 2001), and ~2.55–2.95 Ga crust in the Arabian Shield of Yemen (Whitehouse *et al.* 1998). The eastern Saharan Metacraton also contains Palaeoproterozoic and Archaean crustal components (e.g. Küster *et al.* 2008; Bea *et al.* 2011; Kongnyuy *et al.* 2012; Zhang *et al.* 2019b) and thus can be seen as a possible source area. This may be supported by the fact that the eastern and southeastern parts of the Saharan Metacraton were exposed at the surface and thus were prone to erosion throughout most of the Palaeozoic, according to palaeogeographic reconstructions (e.g. Torsvik & Cocks, 2013).

Although Palaeo- and Eoarchaean zircon ages make up only 0.6% of the obtained concordant age spectrum (Fig. 5), they are of great interest, as pre-3.2 Ga crust is not known from anywhere in the surrounding area (e.g. Hargrove *et al.* 2006; Stern *et al.* 2010; Fritz *et al.* 2013; Johnson, 2014). The exception is uppermost Palaeoarchaean basement rock in southwest Egypt, i.e. 3.22 ± 0.02 Ga gneiss at Gebel Kamil (Bea *et al.* 2011) and 3.245 ± 0.05 Ga gneiss at Gebel Uweinat (Zhang *et al.* 2019b). The Devonian samples yielded the highest amount of Palaeo- and Eoarchaean zircon ages compared to all other studied samples and surprisingly, they yielded the oldest zircon ages yet recorded from Arabia and the surrounding area: 3771 ± 37 Ma (#: 82) and 3850 ± 25 Ma (#: 38) in the Jubah Formation sample 152 (Figs 4, 5). Similar old ages (3729–3769 Ma, n = 4) were reported from inherited zircon crystals in Neogene ignimbrites of Central Anatolia in Turkey, and it was suggested to be an indication for the presence of Early Archaean basement in the Anatolian subsurface (Paquette & Le Pennec, 2012, 2013). However, an alternative explanation such as derivation from a Gondwanan source and later reworking by sedimentary and/or igneous events has been put forward (Köksal *et al.* 2013). Nutman *et al.* (2014) reported an inherited zircon core of 3579 Ma from a Pan-African granite of the Sanandaj–Sirjan Zone and discussed it as the oldest crustal material yet found in Iran. The source of these old grains is not yet known. Archaean zircons may represent xenocrystic zircons assimilated from terrigenous sediment, may reflect assimilation of cryptic Archaean continental crust that underlies the juvenile crust of the Arabian–Nubian Shield (Hargrove *et al.* 2006), or may indicate a more distal source area such as the Saharan Metacraton. It can be speculated that yet unknown terrigenous sediment and/or igneous rocks containing inherited up to Eoarchaean components may occur in the Saharan Metacraton. These rocks were later eroded, and the detrital material was transported by continental-scale river systems and/or glaciers toward the Arabian Peninsula.

5.b. Sample comparison

Multidimensional scaling (MDS) has successfully been applied to detrital zircon age datasets from Palaeozoic sandstones of northern Gondwana (Stephan *et al.* 2019a; Lewin *et al.* 2020a) and is applied here to Palaeozoic sandstones from Saudi Arabia (Section 5.b.1), followed by a comparison with samples from Ethiopia (Section 5.b.2.). However, it is worth keeping in

mind that quantitative comparisons of U–Pb age distributions can be biased because, for example, there is a grain-size dependence on age-data acquisition and interpretation (e.g. Yang *et al.* 2012; Ibañez-Mejia *et al.* 2018).

5.b.1. Comparison of samples from Saudi Arabia

First, among the samples from Saudi Arabia, the Cambrian and Ordovician samples (Fig. 8a) are separately discussed from the Devonian to Permian samples (Fig. 8b) before discussing all samples in a single MDS plot (Fig. 8c). Among the Cambrian and Ordovician samples, there is no clear separation according to stratigraphic age or study area, i.e. Wajid versus Tabuk. However, among the Wajid samples, the Cambrian–Ordovician Dibsiyah Formation samples (74 and 79) differ from those of the Upper Ordovician Sanamah Formation (62 and 73), and the two samples from the Sanamah Formation are very similar in their zircon spectra (Fig. 8a). The Cambrian–Ordovician Saq Formation sample 169 from the Tabuk area shows some resemblance to the Cambrian–Ordovician Dibsiyah Formation sample 74 of the Wajid area whereas the Cambrian–Ordovician Saq Formation sample 170 from the Tabuk area shows the least similarity to the Cambrian–Ordovician Dibsiyah Formation of the Wajid area (Fig. 8a). The Ordovician Qasim Formation samples from the Tabuk area form two sample groups. Group 1 comprises the older samples 144/1 and 145 whereas group 2 comprises the younger samples 124 and 126 (Figs 7, 8a). Overall, these patterns among the Cambrian and Ordovician samples suggest times of a homogeneous sediment source and times of sediment supply from different sources to the Wajid and Tabuk areas.

Among the Devonian to Permian samples, there is a clear separation according to stratigraphic age, Devonian versus Carboniferous–Permian, but not according to the study area, i.e. Wajid versus Tabuk (Fig. 8b). Thus, during the Devonian the sediment provenance was relatively similar for both the Wajid and Tabuk areas. The sediment source changed in the Carboniferous–Permian but again it was similar throughout both study areas.

Comparing the Devonian to Permian samples with the Cambrian and Ordovician samples in an MDS plot reveals some interesting similarities (Fig. 8c). According to that, zircon populations of the Upper Palaeozoic sandstones resemble those of the Lower Palaeozoic sandstones in both study areas. However, the Upper Palaeozoic sandstone composition can not simply be explained by sediment recycling of Lower Palaeozoic sandstones because the latter are mainly quartz arenites (Fig. 3b) with a dominance of zircon, tourmaline and rutile among the transparent heavy minerals (Babalola, 1999; Hussain *et al.* 2004; Knox *et al.* 2007; Bassis *et al.* 2016b) whereas the Upper Palaeozoic are more feldspar rich (Fig. 3b) and also contain unstable transparent heavy minerals like garnet and/or staurolite (e.g. Knox *et al.* 2007; Bassis *et al.* 2016b). Thus, it is more likely that fresh basement rocks with zircon ages resembling that from basement rocks, which supplied sediment to the Lower Palaeozoic sandstones also supplied detritus to the Upper Palaeozoic sandstones. Minor sediment recycling from Lower Palaeozoic sandstones may have occurred but certainly, it cannot account for the majority of the detrital material in the Upper Palaeozoic sandstones.

5.b.2. Comparison of samples from Saudi Arabia with those from Ethiopia

In Ethiopia, Palaeozoic successions are present around the Mekelle Basin in the Tigray province of northern Ethiopia and, to a minor extent, in the Blue Nile region in the west of the country and comprise of Upper Ordovician and Carboniferous–Permian glaciogenic sandstones (e.g. Lewin *et al.* 2018, and references therein). Comparing detrital zircon data from Upper Ordovician sandstones of Ethiopia (Lewin *et al*. 2020a) with those from Saudi Arabia (this study) in an MDS plot reveals that Upper Ordovician samples from the Wajid area resemble those from northern Ethiopia whereas Upper Ordovician samples from the Tabuk area resemble those from northernmost Ethiopia (Fig. 9). The slight dissimilarity of the

age spectra among the glaciogenic sandstones leads to the assumption that a change in provenance occurred during the Late Ordovician (Hirnantian) glaciation. Overall, however, the high similarity of many of the Cambrian–Ordovician age spectra with those of the Upper Ordovician glaciogenic sandstones (Fig. 8a) suggests that no change in provenance occurred with the onset of glaciation. Rather, the glaciers reworked sediment from the underlying Cambrian to Middle Ordovician successions to account for the high maturity of the Upper Ordovician siliciclastics (e.g. Lewin *et al.* 2018, 2020a, 2020b). Thus, large-scale sediment recycling occurred across northeast Africa and Arabia during the Hirnantian Gondwana glaciation.

The Carboniferous–Permian samples from Ethiopia plot distinct to those from Saudi Arabia but with one sample from each of the Wajid and Tabuk areas being close to those from Ethiopia (Fig. 10). Carboniferous–Permian glaciogenic sandstones from Ethiopia and Saudi Arabia show a similar sediment composition, i.e. being feldspar bearing and containing unstable heavy minerals (Bassis *et al.* 2016a,b; Lewin *et al.* 2018, 2020b). The detritus of the Carboniferous–Permian glaciogenic sandstones of Ethiopia was probably derived from the south, i.e. from basement rocks of the Nubian Shield as inferred from detrital zircon data (Lewin *et al.* 2020a), and a northward transport direction was inferred by Bussert (2010) based on the orientation and geometry of palaeolandforms, such as roches moutonnées (Lewin *et al.* 2020a). In northern Ethiopia, the glaciogenic sandstones were deposited in a large NNE-trending trough in which glacial erosion may have followed and reinforced this preglacial topography (Lewin *et al.* 2020a). Before the opening of the Red Sea, the Arabian Peninsula was attached to northeast Africa (Fig. 1b), and thus the Wajid area was in proximity to Ethiopia. Taking all data together, it is suggested that the Carboniferous–Permian glaciogenic sandstones of Saudi Arabia received the majority of their detritus due to erosion of fresh basement rocks likely from the Nubian Shield such as in Ethiopia. On their way to the northeast, only minor amounts of detritus were admixed from the Arabian Shield.

5.c. Gondwana super-fan system and East African–Arabian zircon province

Based on the similarity of detrital zircon U–Pb age spectra in Palaeozoic sandstones throughout Gondwana, Squire *et al.* (2006) postulated the existence of large sediment fans that brought detritus from the East African Orogen towards the continental margins of Gondwana. Meinhold *et al.* (2013) extended the super-fan model to the northern Gondwana margin evaluating detrital zircon age spectra from Cambrian–Ordovician sandstones of Morocco, Algeria, Libya, Israel and Jordon. Sediment belonging to the Gondwana super-fan system contains a prominent amount of ~1 Ga detrital zircons besides grains with ages of ~0.53–0.75, ~1.75–2.15 and ~2.5–2.7 Ga (Meinhold *et al.* 2013). The ~1 Ga zircons are a key feature of the Gondwana super-fan system and were likely transported from regions in the centre of the East African Orogen, i.e. from the Mozambique Belt, or from regions of the southeastern Saharan Metacraton towards the continental margin of Gondwana during the early Palaeozoic. Intensive source area weathering, low sedimentation rates, and reworking during deposition lead to the high mineralogical maturity of the Lower Palaeozoic sediment (see discussion in Bassis *et al.* 2016a) containing ~1 Ga zircons. According to the Gondwana super-fan model, Saudi Arabia would lie more distal along the sediment path to the northeast. Based on a more extensive detrital zircon dataset including also peri-Gondwana units and using multivariate data analysis, Stephan *et al.* (2019a) showed the existence of three contrasting provenance end-members in Lower Palaeozoic sedimentary rocks of the former Gondwanan shelf, namely the Avalonian, West African, and East African–Arabian zircon provinces (see also Stephan *et al.* 2019b). The East African–Arabian zircon province corresponds to the Gondwana super-fan system of Meinhold *et al.* (2013). To test whether the East African–Arabian zircon province is also a feature of the Lower Palaeozoic sandstones of Saudi Arabia, we compared in an MDS plot the newly obtained detrital zircon data from

Saudi Arabia (this study) with those from the literature for north and northeast Africa, Israel and Jordon (Fig. 11).

The majority of the Lower Palaeozoic samples from Saudi Arabia reveals a high similarity to samples from Libya, Israel, Jordan, and Ethiopia (Fig. 11). This suggests that the Gondwana super-fan system was extensive and supplied detritus with a signature of an East African–Arabian zircon province also to the Lower Palaeozoic succession of Saudi Arabia (Fig. 12). The Algerian samples are not part of the cluster. In addition, some Cambrian and Lower Ordovician samples from Libya, Israel and Jordan are not part of the cluster. This is because the Gondwana super-fan system with an East African–Arabian zircon province seems to have been active at different times across northeast Africa and Arabia, with the main phase of activity starting at some point between the Late Cambrian and late Middle Ordovician (Meinhold *et al.* 2013).

As discussed in Section 5.a., the Sa'al metamorphic complex on the Sinai Peninsula comprises ~1 Ga basement rocks (Be'eri-Shlevin *et al.* 2012) and it is in proximity to the study area, at least to the Tabuk area. However, sediment supply from the Sinai basement to the Ordovician succession of Saudi Arabia is rather unlikely taking into account the roundness of the detrital zircon grains (this study) and the palaeocurrent data that point toward a southerly provenance (Dabbagh & Rogers, 1983; Stump & van der Eem, 1995; Babalola, 1999; Hussain *et al.* 2000). For example, palaeocurrents of Upper Ordovician sandstones from the southeastern Tabuk area show sediment transport away from the Arabian Shield toward the northeast (Clark-Lowes, 2005).

6. Conclusions

The erosion history of the East African Orogen and sediment recycling in northern Gondwana during the Palaeozoic have been topics of much debate. Our new detrital zircon U–Pb ages from 24 sandstone samples from the Cambrian to Permian succession of Saudi Arabia provide new insights into these topics.

Five main zircon age populations have been identified in varying amounts, with age peaks at ~625 Ma, ~775 Ma, ~980 Ma, ~1840 Ma, and ~2480 Ma. Igneous rocks are the primary source of these grains, as most of the zircons show undisturbed oscillatory zoning and some also showing regrowth features in the CL images. Ediacaran to middle Tonian zircon grains are likely derived from igneous rocks of the Arabian–Nubian Shield. Palaeoproterozoic and Archaean grains may be xenocrystic zircons. However, this likely only accounts for a small number of grains. Recycling from older terrigenous sediment is possible. A primary derivation from Palaeoproterozoic and Archaean basement is also likely, as meta-igneous rocks of such age occur in the vicinity of the study area. A minor amount (4%) of the detrital zircons show Palaeozoic (340–541 Ma) ages. Early Palaeozoic zircons are likely derived from Cambrian and Ordovician post-orogenic igneous rocks, as present in the Arabian–Nubian Shield and to the south. Late Palaeozoic zircons may come from within-plate, anorogenic igneous rocks, as known from northern Arabia.

It is worth emphasising that the zircon grains with up to Eoarchean (3.6–4.0 Ga) ages are the oldest zircons yet presented from Arabia and its vicinity. It can be speculated that these grains represent xenocrystic cores originally derived from igneous rocks of the Arabian–Nubian Shield. However, such old ages have not yet been described from basement rocks of northeast Africa and Arabia and thus their origin is enigmatic. Tonian–Stenian (900 to <1200 Ma) zircons are present in varying amounts in all of the samples and are a feature of terrigenous sediment belonging to the Gondwana super-fan system and the East African–Arabian zircon province, respectively, in early Palaeozoic time. Multi-dimensional scaling (MDS) reveals similarities between detrital zircon age spectra from Ordovician sandstones of Saudi Arabia with time equivalent successions of Ethiopia, Libya, Israel and Jordon. Thus, the Gondwana super-fan system with an East African–Arabian zircon province had a larger

size than previously thought, as it also reached the Arabian Peninsula during the early Palaeozoic. Glaciogenic sandstones from Saudi Arabia related to the Late Ordovician (Hirnantian) Gondwana glaciation resemble time equivalent successions from Ethiopia, suggesting prominent sediment transport and recycling with similar provenance. Besides that, MDS shows dissimilarities between detrital zircon spectra from Devonian and Carboniferous–Permian sandstones of Saudi Arabia, suggesting a prominent provenance change with the onset of the late Palaeozoic Gondwana glaciation.

Acknowledgements. This work was supported by the German Research Foundation (DFG grant numbers HI 643/13-1, ME 3882/4-1). We thank the logistical support of the Deutsche Gesellschaft für Internationale Zusammenarbeit (GIZ) GmbH and Dornier Consulting International (DCo) GmbH in Riyadh. A special thanks goes to Randolf Rausch and the entire GIZ/DCo staff for their assistance and support during the field campaign and their interest in this study. We are grateful to Andreas Kronz for providing access to the electron microprobe for cathodoluminescence imaging and to Beate Schmitte for assistance at the laser ablation inductively coupled plasma mass spectrometry facility. Careful and constructive reviews by Victoria Pease and an anonymous reviewer are greatly appreciated.

Declaration of Interest. None.

Supplementary Material. To view supplementary material for this article, please visit https://doi.org/xxxxxxxx

References

Agar RA, Stacey JS and Whitehouse MJ (1992) Evolution of the southern Afif terrane—A geochronologic study. *Saudi Arabian Directorate General of Mineral Resources, Open-File Report* **DGMR-OF-10-15**, 1–41.

Al-Ajmi HF, Keller M, Hinderer M and Filomena CM (2015) Lithofacies, depositional environments and stratigraphic architecture of the Wajid Group outcrops in southern Saudi Arabia. *GeoArabia* **20**, 49–94.

Al-Harbi OA and Khan MM (2008) Provenance, diagenesis, tectonic setting and geochemistry of Tawil Sandstone (Lower Devonian) in Central Saudi Arabia. *Journal of Asian Earth Sciences* **33**, 278–87.

Al-Harbi OA and Khan MM (2011) Source and origin of glacial paleovalley-fill sediments (Upper Ordovician) of Sarah Formation in central Saudi Arabia. *Arabian Journal of Geosciences* **4**, 825–35.

Ali KA, Stern RJ, Manton WI, Johnson PR and Mukherjee SK (2010) Neoproterozoic diamictite in the Eastern Desert of Egypt and Northern Saudi Arabia: evidence of 750 Ma glaciation in the Arabian–Nubian Shield. *International Journal of Earth Sciences* **90**, 705–26.

Altumi MM, Elicki O, Linnemann U, Hofmann M, Sagawe A and Gärtner A (2013) U–Pb LA-ICP-MS detrital zircon ages from the Cambrian of Al Qarqaf Arch, central-western Libya: provenance of the West Gondwanan sand sea at the dawn of the early Palaeozoic. *Journal of African Earth Sciences* **79**, 74–97.

Alsharhan AS, Nairn AEM and Mohammed AA (1993) Late Palaeozoic glacial sediments of the southern Arabian Peninsula: their lithofacies and hydrocarbon potential. *Marine and Petroleum Geology* **10**, 71–8.

Avigad D, Sandler A, Kolodner K, Stern R, McWilliams M, Miller N and Beyth M (2005) Mass-production of Cambro–Ordovician quartz-rich sandstone as a consequence

of chemical weathering of Pan-African terranes: environmental implications. *Earth and Planetary Science Letters* **240**, 818–26.

Avigad D, Stern RJ, Beyth M, Miller N and McWilliams MO (2007) Detrital zircon U–Pb geochronology of Cryogenian diamictites and Lower Paleozoic sandstone in Ethiopia (Tigrai): Age constraints on Neoproterozoic glaciation and crustal evolution of the southern Arabian–Nubian Shield. *Precambrian Research* **154**, 88–106.

Avigad D, Gerdes A, Morag N and Bechstädt T (2012) Coupled U–Pb–Hf of detrital zircons of Cambrian sandstones from Morocco and Sardinia: implications for provenance and Precambrian crustal evolution of North Africa. *Gondwana Research* **21**, 690–703.

Avigad D, Morag N, Abbo A and Gerdes A (2017) Detrital rutile U–Pb perspective on the origin of the great Cambro-Ordovician sandstone of North Gondwana and its linkage to orogeny. *Gondwana Research* **51**, 17–29.

Babalola LO (1999) Depositional Environments and Provenance of the Wajid Sandstone, Abha-Khamis Mushayt Area. MSc Thesis, King Fahd University of Petroleum and Minerals, Dhahran, Saudi Arabia, Southwestern Saudi Arabia.

Bassis A, Hinderer M and Meinhold G (2016a) Petrography and geochemistry of Palaeozoic quartz-rich sandstones from Saudi Arabia: implications for provenance and chemostratigraphy. *Arabian Journal of Geosciences* **9**, 400, doi: 10.1007/s12517-016-2412-z.

Bassis A, Hinderer M and Meinhold G (2016b) New insights into the provenance of Saudi Arabian Palaeozoic sandstones from heavy mineral analysis and single-grain geochemistry. *Sedimentary Geology* **333**, 100–14.

Bea F, Montero P, Abu Anbar M and Talavera C (2011) SHRIMP dating and Nd isotope geology of the Archean terranes of the Uweinat-Kamil inlier, Egypt–Sudan–Libya. *Precambrian Research* **189**, 328–46.

Be'eri-Shlevin Y, Katzir Y, Whitehouse MJ and Kleinhanns CI (2009) Contribution of pre Pan-African crust to formation of the Arabian Nubian Shield: New secondary ionization mass spectrometry U–Pb and O studies of zircon. *Geology* **37**, 899–902.

Be'eri-Shlevin Y, Eyal M, Eyal Y, Whitehouse MJ and Litvinovsky B (2012) The Sa'al volcano-sedimentary complex (Sinai, Egypt), a latest Mesoproterozoic volcanic arc in the northern Arabian Nubian Shield. *Geology* **40**, 403–6.

Bishop RS (1995) Maturation history of the lower Palaeozoic of the eastern Arabian Platform. In *Middle East Petroleum Geosciences, GEO'94* (ed MI Al-Husseini), pp. 180–189. Gulf PetroLink, Manama, Bahrain no. 1.

Burke K, MacGregor DS and Cameron NR (2003) Africa's petroleum systems: four tectonic 'Aces' in the past 600 million years. In *Petroleum Geology of Africa: New Themes and Developing Technologies* (eds TJ Arthur, DS MacGregor and NR Cameron), pp. 21–60. Geological Society of London, Special Publication no. 207.

Bussert R (2010) Exhumed erosional landforms of the Late Palaeozoic glaciation in northern Ethiopia: indicators of ice-flow direction, palaeolandscape and regional ice dynamics. *Gondwana Research* **18**, 356–69.

Clark-Lowes DD (2005) Arabian glacial deposits: recognition of palaeovalleys within the Upper Ordovician Sarah Formation, Al Qasim district, Saudi Arabia. *Proceedings of the Geologists' Association* **116**, 331–47.

Cohen KM, Harper DAT, Gibbard PL and Fan J-X (2018) The International Chronostratigraphic Chart. International Commission on Stratigraphy, http://www.stratigraphy.org/ICSchart/ChronostratChart2018-08.pdf

Corfu F, Hanchar JM, Hoskin PWO and Kinny P (2003) Atlas of zircon textures. In *Zircon* (eds JM Hanchar and PWO Hoskin), pp. 469–500. Reviews in Mineralogy and Geochemistry no. 53.

Dabbagh ME and Rogers JJW (1983) Depositional environments and tectonic significance of the Wajid Sandstone of Saudi Arabia. *Journal of African Earth Sciences* **1**, 47–57.
Dickinson WR and Gehrels GE (2009) Use of U–Pb ages of detrital zircons to infer maximum depositional ages of strata: a test against a Colorado Plateau Mesozoic database. *Earth and Planetary Science Letters* **288**, 115–25.
Fritz H, Abdelsalam M, Ali KA, Bingen B, Collins AS, Fowler AR, Ghebreab W, Hauzenberger CA, Johnson PR, Kusky TM, Macey P, Muhongo S, Stern RJ and Viola G (2013) Orogen styles in the East African Orogen: A review of the Neoproterozoic to Cambrian tectonic evolution. *Journal of African Earth Sciences* **86**, 65–106.
Garfunkel Z (2002) Early Paleozoic sediments of NE Africa and Arabia: products of continental-scale erosion, sediment transport and deposition. *Israel Journal of Earth Sciences* **51**, 135–56.
Garzanti E, Vermeesch P, Andò S, Vezzoli G, Valagussa M, Allen K, Kadi KA and Al-Juboury AIA (2013) Provenance and recycling of Arabian desert sand. *Earth-Science Reviews* **120**, 1–19.
Golan T, Katzir Y and Coble MA (2018) Early Carboniferous anorogenic magmatism in the Levant: implications for rifting in northern Gondwana. *International Geology Review* **60**, 101–8.
Hargrove US, Stern RJ, Kimura J-L, Manton WI and Johnson PR (2006) How juvenile is the Arabian–Nubian Shield? Evidence from Nd isotopes and pre-Neoproterozoic inherited zircon from the Bi'r Umq suture zone, Saudi Arabia. *Earth and Planetary Science Letters* **252**, 308–26.
Haq BU and Schutter SR (2008) A chronology of Paleozoic sea-level changes. *Science* **322** (5898), 64–8.
Hinderer M, Keller M, Al-Ajmi H and Rausch R (2009) Tales of two glaciations in the Paleozoic of SW Saudi Arabia: implications for ice shield dynamics and paleogeography of the SW Arabian Platform and adjacent areas. 5th Workshop of the ILP Task Force on Sedimentary Basins, 6-11 December 2009, Abu Dhabi, United Arab Emirates.
Höhndorf A, Meinhold K-D and Vail JR (1994) Geochronology of anorogenic igneous complexes in the Sudan—isotopic investigations in north Kordofan, the Nubian Desert and the Red-Sea Hills. *Journal of African Earth Sciences* **19**, 3–15.
Hubert JF (1962) A zircon–tourmaline–rutile maturity index and the interdependence of the composition of heavy mineral assemblages with the gross composition and texture of sandstones. *Journal of Sedimentary Petrology* **32**, 440–50.
Hussain M, Babalola LO and Hariri M (2000) Provenance of the Wajid Sandstone, southeastern margin of the Arabian shield: geochemical and petrographic approach. *American Association of Petroleum Geologists National Conference, New Orleans, USA, April 16, 1999.*
Hussain M, Babalola LO and Hariri MM (2004) Heavy minerals in the Wajid Sandstone from Abha-Khamis Mushayt area, southwestern Saudi Arabia: implications on provenance and regional tectonic setting. *GeoArabia* **9**, 77–102.
Ibañez-Mejia M, Pullen A, Pepper M, Urbani F, Ghoshal G and Ibañez-Mejia JC (2018) Use and abuse of detrital zircon U-Pb geochronology—A case from the Río Orinoco delta, eastern Venezuela. *Geology* **46**, 1019–22.
Johnson PR (2014) An expanding Arabian-Nubian Shield geochronologic and isotopic dataset: defining limits and confirming the tectonic setting of a Neoproterozoic accretionary orogen. *The Open Geology Journal* **8**, 3–33.
Johnson PR, Andresen A, Collins AS, Fowler AR, Fritz H, Ghebreab W, Kusky T and Stern RJ (2011) Late Cryogenian–Ediacaran history of the Arabian–Nubian Shield: a

review of depositional, plutonic, structural, and tectonic events in the closing stages of the northern East African Orogen. *Journal of African Earth Sciences* **61**, 167–232.

Johnson PR, Halverson GP, Kusky TM, Stern RJ and Pease V (2013) Volcanosedimentary Basins in the Arabian-Nubian Shield: Markers of Repeated Exhumation and Denudation in a Neoproterozoic Accretionary Orogen. *Geosciences* **3**, 389–445.

Keller M, Hinderer M, Al-Ajmi HF and Rausch R (2011) Palaeozoic glacial depositional environments of SW Saudi Arabia: process and product. In *Ice-marginal and Periglacial Processes and Sediments* (eds IP Martini, HM French and A Pérez Alberti), pp. 129–52. Geological Society of London, Special Publication no. 354.

Kolodner K, Avigad D, McWilliams M, Wooden JL, Weissbrod T and Feinstein S (2006) Provenance of north Gondwana Cambrian–Ordovician sandstone: U–Pb SHRIMP dating of detrital zircons from Israel and Jordan. *Geological Magazine* **143**, 367–91.

Kongnyuy SC, Giulio M and Satir M (2012) Archaean zircon U-Pb age paradox in juvenile Neoproterozoic granitoids, Central North Sudan, Saharan Metacraton. *Turkish Journal of Earth Sciences* **21**, 97–125.

Köksal S, Toksoy-Köksal F, Göncüoglu MC, Möller A, Gerdes A and Frei D (2013) 3.8 Ga zircons sampled by Neogene ignimbrite eruptions in Central Anatolia: COMMENT. *Geology* **41**(12), e307.

Knox RWO'B, Franks SG and Cocker JD (2007) Stratigraphic evolution of heavy-mineral provenance signatures in the sandstones of the Wajid Group (Cambrian to Permian), southwestern Saudi Arabia. *GeoArabia* **12**, 65–96.

Kooijman E, Berndt J and Mezger K (2012) U–Pb dating of zircon by laser ablation ICP-MS: recent improvements and new insights. *European Journal of Mineralogy* **24**, 5–21.

Kröner A 1985. Ophiolites and the evolution of tectonic boundaries in the late Proterozoic Arabian–Nubian shield of northeast Africa and Arabia. *Precambrian Research* **27**, 277–300.

Kröner A, Stern RJ, Dawoud AS, Compston W and Reischmann T (1987) The Pan-African continental margin in northeastern Africa: evidence from a geochronological study of granulites at Sabaloka, Sudan. *Earth and Planetary Science Letters* **85**, 91–104.

Küster D, Liégeois J-P, Matukov D, Sergeev S and Lucassen F (2008) Zircon geochronology and Sr, Nd, Pb isotope geochemistry of granitoids from Bayuda Desert and Sabaloka (Sudan): evidence for a Bayudian event (920–900 Ma) preceding the Pan-African orogenic cycle (860–590 Ma) at the eastern boundary of the Saharan Metacraton. *Precambrian Research* **164**, 16–39.

Laboun AA (2010) Paleozoic tectono-stratigraphic framework of the Arabian Peninsula. *Journal of King Saud University (Science)* **22**, 41–50.

Linnemann U, Ouzegane K, Drareni A, Hofmann M, Becker S, Gärtner A and Sagawe A (2011) Sands of West Gondwana: an archive of secular magmatism and plate interactions — a case study from the Cambro-Ordovician section of the Tassili Ouan Ahaggar (Algerian Sahara) using U–Pb–LA-ICP-MS detrital zircon ages. *Lithos* **123**, 188–203.

Lewin A, Meinhold G, Hinderer M, Dawit EL and Bussert R (2018) Provenance of sandstones in Ethiopia during Late Ordovician and Carboniferous–Permian Gondwana glaciations: petrography and geochemistry of the Enticho Sandstone and the Edaga Arbi Glacials. *Sedimentary Geology* **375**, 188–202.

Lewin A, Meinhold G, Hinderer M, Dawit EL, Bussert R and Berndt J (2020a) Provenance of Ordovician–Silurian and Carboniferous–Permian glaciogenic successions in Ethiopia revealed by detrital zircon U–Pb geochronology. *Journal of the Geological Society, London* **177**, 141–52.

Lewin A, Meinhold G, Hinderer M, Dawit EL, Bussert R and Lünsdorf NK (2020b) Heavy minerals as provenance indicator in glaciogenic successions: An example from the Palaeozoic of Ethiopia. *Journal of African Earth Sciences* **165**, 103813, doi: 10.1016/j.jafrearsci.2020.103813.

Löwen K, Meinhold G, Güngör T and Berndt J (2017) Palaeotethys-related sediments of the Karaburun Peninsula, western Turkey: constraints on provenance and stratigraphy from detrital zircon geochronology. *International Journal of Earth Sciences* **106**, 2771–96.

McClure HA (1980) Permian-Carboniferous glaciation in the Arabian Peninsula. *Geological Society of America Bulletin* **91**, 707–12.

Meinhold G, Morton AC, Fanning CM, Frei D, Howard JP, Phillips RJ, Strogen D and Whitham AG (2011) Evidence from detrital zircons for recycling of Mesoproterozoic and Neoproterozoic crust recorded in Paleozoic and Mesozoic sandstones of southern Libya. *Earth and Planetary Science Letters* **312**, 164–75.

Meinhold G, Morton AC and Avigad D (2013) New insights into peri-Gondwana paleogeography and the Gondwana super-fan system from detrital zircon U–Pb ages. *Gondwana Research* **23**, 661–65.

Morag N, Avigad D, Gerdes A, Belousova E and Harlavan Y (2011) Detrital zircon Hf isotopic composition indicates long-distance transport of North Gondwana Cambrian–Ordovician sandstones. *Geology* **39**, 955–58.

Morton AC, Whitham A, Howard J, Fanning M, Abutarruma Y, El Dieb M, Elkatarry FM, Hamhoom AM, Lüning S, Phillips R and Thusu B (2012) Using heavy minerals to test the stratigraphic framework of Al Kufrah Basin. In *Fourth Symposium on the Sedimentary Basins of Libya* (eds MJ Salem and AM Abadi), pp. 33–76. *The Geology of Southern Libya*, Vol. 3, Tripoli: Earth Science Society of Libya.

Nutman AP, Mohajjel M, Bennett VC and Fergusson CL (2014) Gondwanan Eoarchean–Neoproterozoic ancient crustal material in Iran and Turkey: zircon U–Pb–Hf isotopic evidence. *Canadian Journal of Earth Sciences* **51**, 272–85.

Paquette JL and Le Pennec JL (2012) 3.8 Ga zircons sampled by Neogene ignimbrite eruptions in Central Anatolia. *Geology* **40**, 239–42.

Paquette JL and Le Pennec JL (2013) 3.8 Ga zircons sampled by Neogene ignimbrite eruptions in Central Anatolia: REPLY. *Geology* **41**(12), e308.

Pollastro RM, Karshbaum AS and Viger RJ (1998) Maps showing geology, oil and gas fields and geologic provinces of the Arabian Peninsula. *United States Geological Survey, Open-file Report* **97-470B**, 1–14.

Powers RW (1968) Saudi Arabia. In *Lexique Stratigraphique International* (ed L Dubertret), pp. 1–177. *Centre National de la Recherche Scientifique, Paris*, vol. III, Asie.

Powers RW, Ramirez LF, Redmond CD and Elberg Jr EL (1966) Geology of the Arabian Peninsula: sedimentary geology of Saudi Arabia. *United States Geological Survey*, *Professional Paper* **560(D)**, 1–147.

Ramos E, Navidad M, Marzo M and Bolatti N (2003) Middle Ordovician K-bentonite beds in the Murzuq Basin (Central Libya). In *Ordovician from the Andes* (eds GL Albanesi, MS Beresi and SH Peralta), pp. 203–7. Instituto Superior de Correlación Geológica, Universidad Nacional de Tucumán, Tucumán. Serie Correlación Geológica no. 17.

Sharland PR, Archer R, Casey DM, Davies RB, Hall SH, Heward AP, Horbury AD and Simmons MD (2001) Arabian Plate sequence stratigraphy. *GeoArabia*, *Special Publication* **2**, 1–371.

Spencer CJ, Kirkland CL and Taylor RJM (2016) Strategies towards statistically robust interpretations of in situ U–Pb zircon geochronology. *Geoscience Frontiers* **7**, 581–9.

Squire RJ, Campbell IH, Allen CM and Wilson CJL (2006) Did the Transgondwanan Supermountain trigger the explosive radiation of animals on Earth? *Earth and Planetary Science Letters* **250**, 116–33.

Stephan T, Kroner U and Romer RL (2019a) The pre-orogenic detrital zircon record of the Peri-Gondwanan crust. *Geological Magazine* **156**, 281–307.

Stephan T, Kroner U, Romer RL and Rösel D (2019b) From a bipartite Gondwanan shelf to an arcuate Variscan belt: The early Paleozoic evolution of northern Peri-Gondwana. *Earth-Science Reviews* **192**, 491–512.

Stern RJ (1994) Arc assembly and continental collision in the Neoproterozoic East African Orogen: implications for the consolidation of Gondwanaland. *Annual Review of Earth and Planetary Sciences* **22**, 319–51.

Stern RJ, Ali KA, Liégeois J-P, Johnson P, Wiescek F and Kattan F (2010) Distribution and significance of pre-Neoproterozoic zircons in juvenile Neoproterozoic igneous rocks of the Arabian–Nubian Shield. *American Journal of Science* **310**, 791–811.

Stern RJ, Ali KA, Abdelsalam MG, Wilde SA and Zhou Q (2012) U–Pb zircon geochronology of the eastern part of the Southern Ethiopian Shield. *Precambrian Research* **206–207**, 159–67.

Stern RJ, Ren M, Ali K, Förster H-J, Al Safarjalani A, Nasir S, Whitehouse MJ, Leybourne MI and Romer RL (2014) Early Carboniferous (~357 Ma) crust beneath northern Arabia: Tales from Tell Thannoun (southern Syria). *Earth and Planetary Science Letters* **393**, 83–93.

Stump TE and van der Eem JG (1995) The stratigraphy, depositional environments and periods of deforination of the Wajid outcrop belt, southwestern Saudi Arabia. *Journal of African Earth Sciences* **21**, 421–41.

Teklay M, Kröner A, Mezger K and Oberhänsli R (1998) Geochemistry, Pb–Pb single zircon ages and Nd–Sr isotope composition of Precambrian rocks from southern and eastern Ethiopia: implications for crustal evolution in East Africa. *Journal African Earth Sciences* **26**, 207–27.

Torsvik TH and Cocks LRM (2013) Gondwana from top to base in space and time. *Gondwana Research* **24**, 999–1030.

Vermeesch P (2013) Multi-sample comparison of detrital age distributions. *Chemical Geology* **341**, 140–46.

Vermeesch P and Garzanti E (2015) Making geological sense of "Big Data" in sedimentary provenance analysis. *Chemical Geology* **409**, 20–7.

Vermeesch P, Resentini A and Garzanti E (2016) An R package for statistical provenance analysis. *Sedimentary Geology* **336**, 14–25.

Veevers JJ (2007) Pan-Gondwanaland post-collisional extension marked by 650–500 Ma alkaline rocks and carbonatites and related detrital zircons: a review. *Earth-Science Reviews* **83**, 1–47.

Whitehouse MJ, Windley BF, Ba-Bttat MAO, Fanning CM and Rex DC (1998) Crustal evolution and terrane correlation in the eastern Arabian Shield, Yemen: geochronological constraints. *Journal of the Geological Society*, *London* **155**, 281–95.

Whitehouse MJ, Stoeser DB and Stacey JS (2001) The Khida Terrane – geochronological and isotopic evidence for Paleoproterozoic and Archean crust in the eastern Arabian Shield of Saudi Arabia. *Gondwana Research* **4**, 200–2.

Wilde SA and Youssef K (2002) A re-evaluation of the origin and setting of the Late Precambrian Hammamat Group based on SHRIMP U–Pb dating of detrital zircons from Gebel Umm Tawat, North Eastern Desert, Egypt. *Journal of the Geological Society*, *London* **159**, 595–604.

Woolley AR (2001) *Alkaline rocks and carbonatites of the world. Part 3: Africa*. London, Bath: The Geological Society Publishing House, 372 pp.

Yang S, Zhang F and Wang Z (2012) Grain size distribution and age population of detrital zircons from the Changjiang (Yangtze) River system, China. *Chemical Geology* **296–297**, 26–38.

Yibas B, Reimold WU, Armstrong R, Koeberl C, Anhaeusser CR and Phillips D (2002) The tectonostratigraphy, granitoid geochronology and geological evolution of the Precambrian of southern Ethiopia. *Journal of African Earth Sciences* **34**, 57–84.

Zhang W, Pease V, Whitehouse MJ, El-Sankary MM and Shalaby MH (2019a) From the Libyan border to the Nile – Neoproterozoic magmatism and basement evolution of southern Egypt. *International Geology Review* **61**, 2057–79.

Zhang W, Pease V, Whitehouse MJ, El-Sankary MM and Shalaby HM (2019b) Pre-Neoproterozoic basement evolution of southwestern Egypt. *International Geology Review* **61**, 1909–26.

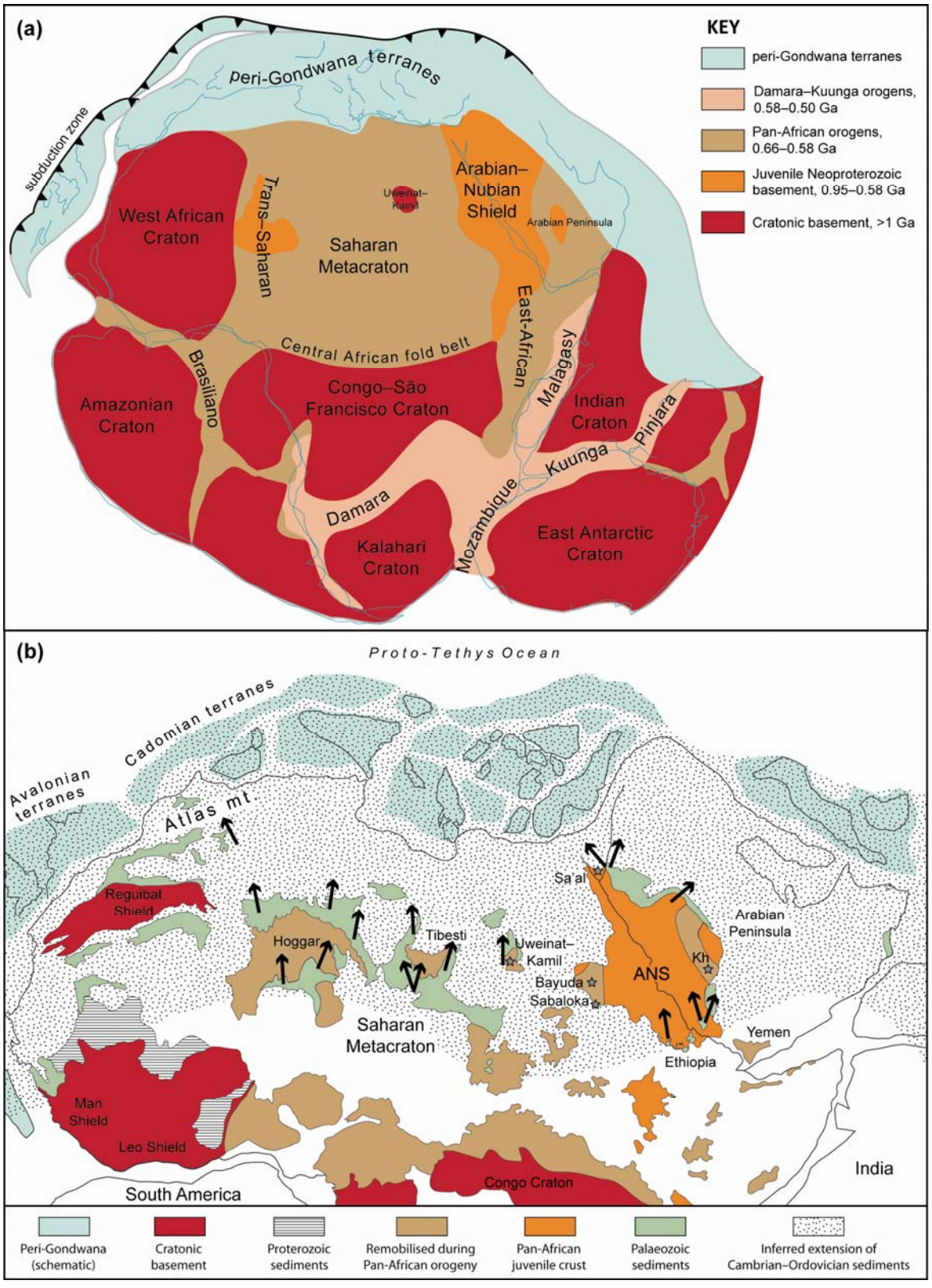

Fig. 1. (Colour online) (a) Reconstruction of Gondwana in the Cambrian showing the main geotectonic units (modified after Avigad *et al.* 2017). (b) Simplified geological map of North Gondwana showing present-day distribution of Precambrian basement rocks and Cambrian–Ordovician sediments (modified after Avigad *et al.* 2012). Black arrows indicate the palaeocurrent directions of Cambrian–Ordovician sediments. Note that for illustration purposes the Red Sea has been closed showing the Arabian–Nubian Shield (ANS) as a single entity. Kh – Khida terrane.

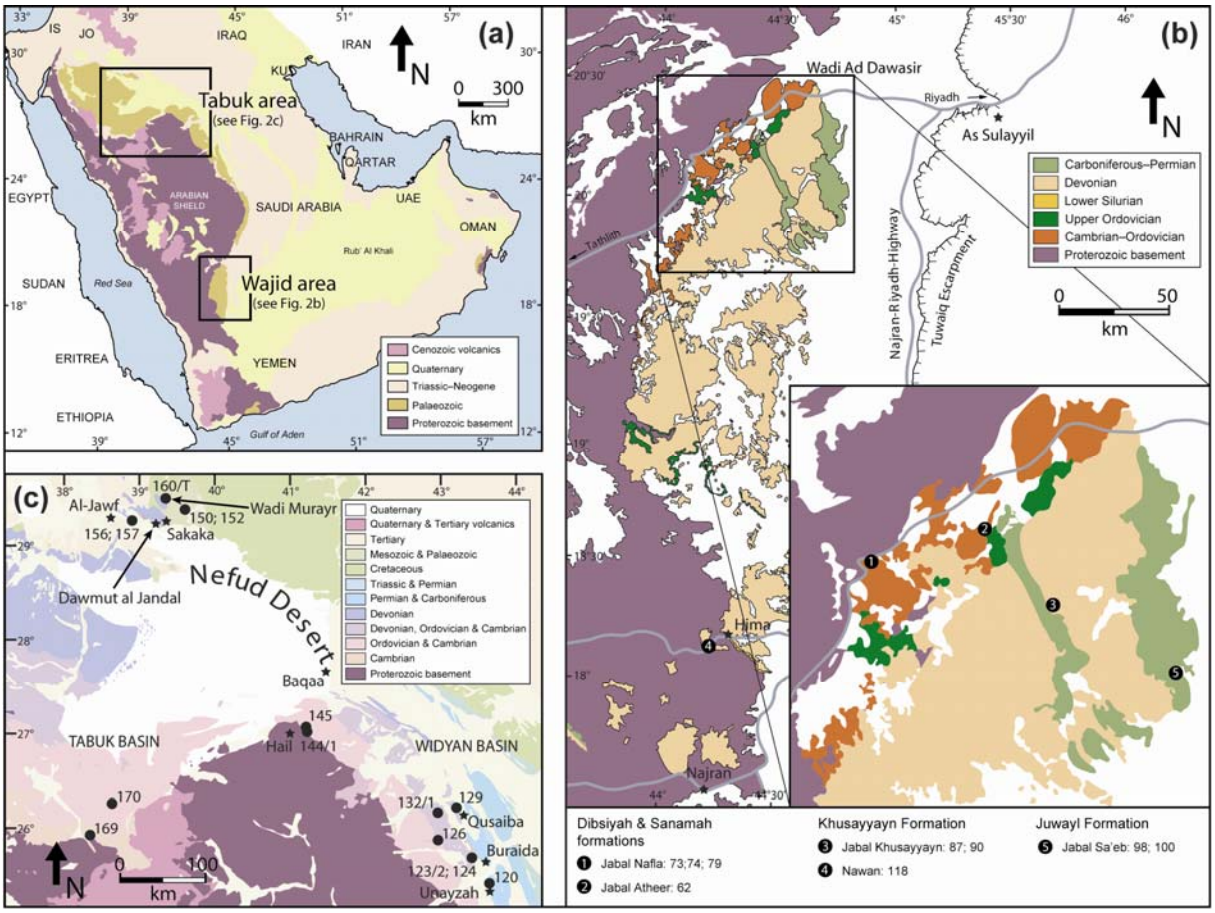

Fig. 2. (Colour online) (a) Simplified geologic map of the Arabian Peninsula showing the study areas (modified after Pollastro *et al.* 1998). For simplification, the Tethyan ophiolite complexes in Oman have been omitted. IS – Israel, JO – Jordan, KU – Kuwait, UAE – United Arab Emirates. (b) Geologic map of the southern Saudi Arabian study area ('Wajid area') (modified after Keller *et al.* 2011). (c) Geologic map of the southern Saudi Arabian study area ('Tabuk area') (modified after Pollastro *et al.* 1998). For simplification, the sample prefix AB-SA has been avoided in the sample localities shown in (b) and (c).

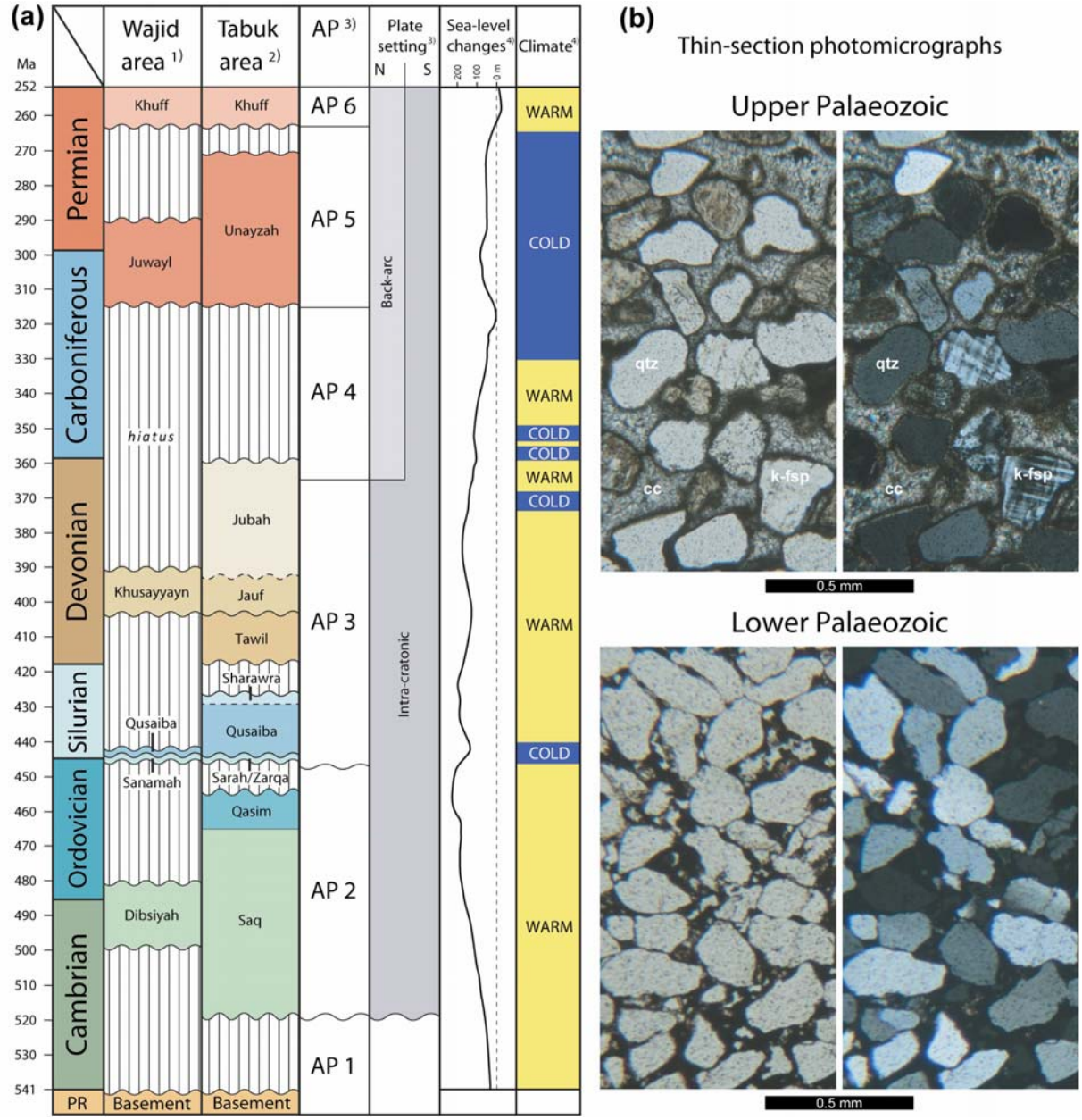

Fig. 3. (Colour online) (a) Simplified stratigraphic column of both study areas. Modified after (1) Al-Ajmi *et al.* (2015), (2) Al-Laboun (2010), (3) Sharland *et al.* (2001) and (4) Haq and Schutter (2008). The dashed vertical line in the column 'Sea-level changes' represents an approximation of the present-day sea level. The column 'Climate' shows time interval with icehouse (cold) and greenhouse (warm) conditions. AP – Arabian plate sequence stratigraphy. PR – Proterozoic. (b) Thin-section photomicrographs of some representative samples from the Palaeozoic succession of Saudi Arabia under regular view (left-hand side) and with crossed polarizers (right-hand side). The Lower Palaeozoic sample is a highly mature and well-sorted quartz arenite from the Dibsiyah Formation (AB-SA79), typical for most of the Palaeozoic succession. The Upper Palaeozoic sample is an arkose from the Juwayl Formation (AB-SA98) with intense calcite cementation. Mineral abbreviations: qtz – quartz; k-fsp – kali-feldspar; cc – calcite. We refer to Bassis *et al.* (2016a,b) for details about the composition and maturity of the Palaeozoic succession of Saudi Arabia and the samples analyzed in this study.

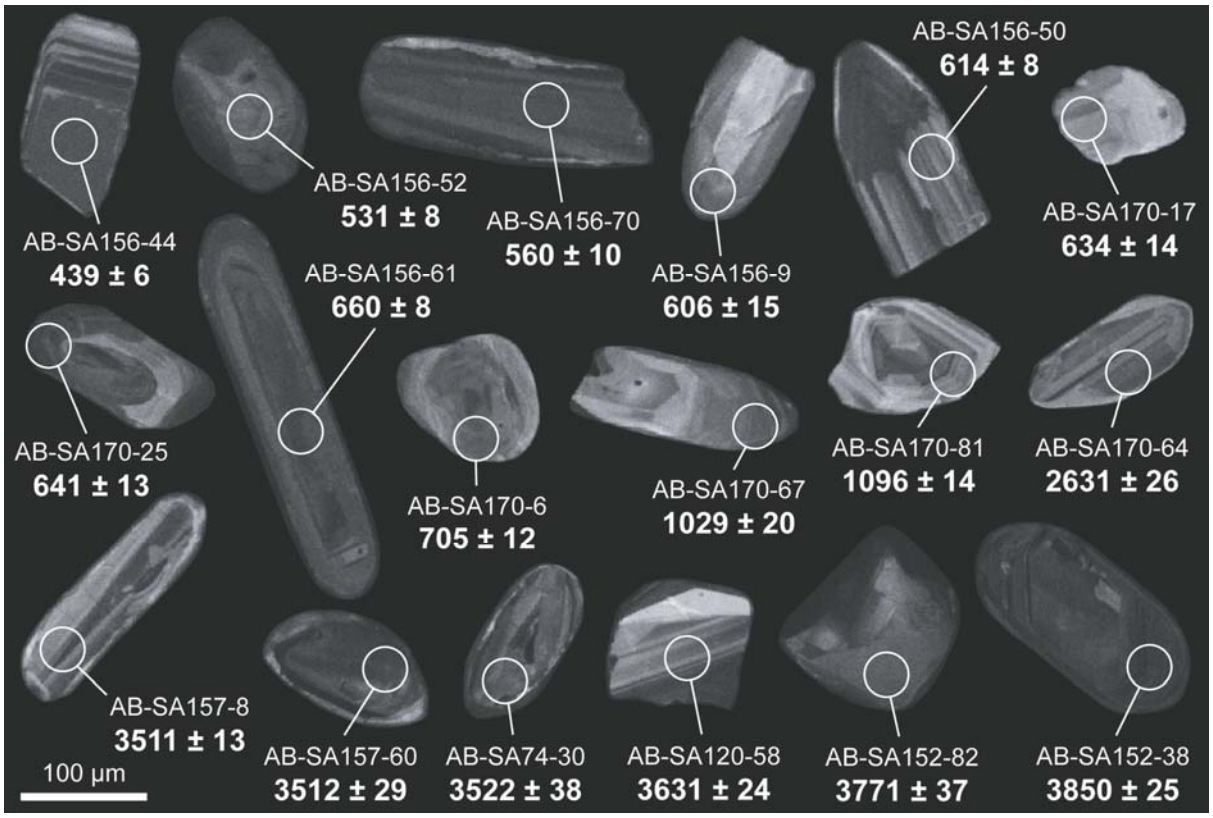

Fig. 4. Cathodoluminescence images of representative zircon grains from samples analysed in this study with the location of the LA–ICP–MS analysis spot and the corresponding $^{206}Pb/^{238}U$ age reported with ±2σ uncertainty in Ma for grains younger than 1.2 Ga and $^{207}Pb/^{206}Pb$ age reported with ±2σ uncertainty in Ma for grains older than 1.2 Ga. The number after the sample name corresponds to the analysis spot as indicated in the Supplementary Table S2.

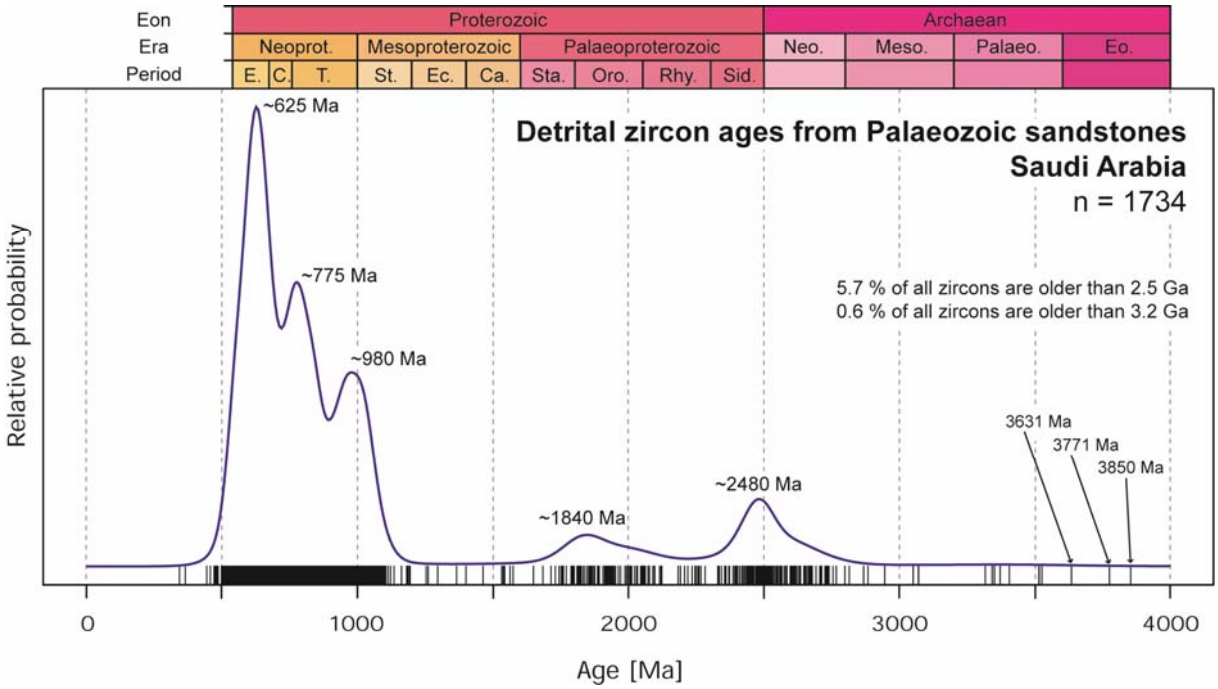

Fig. 5. (Colour online) Kernel density estimate plot showing a summary of U–Pb analytical detrital zircon data for all samples analysed in this study. Only grains with 90 to 110% concordance are shown. n – number of zircon ages. For simplification, and as the majority of the detrital zircons are older than Phanerozoic, no chronostratigraphic subdivisions for Era and Period are shown for the Phanerozoic Eon. Abbreviations of Periods: E. – Ediacaran, C. – Cryogenian, T. – Tonian, St. – Stenian, Ec. – Ectasian, Ca. – Calymmian, Sta. – Statherian, Oro. – Orosirian, Rhy. – Rhyacian, Sid. – Siderian. Abbreviations of Eras: Neoprot. – Neoproterozoic, Neo. – Neoarchaean, Meso. – Mesoarchaean, Palaeo. – Palaeoarchaean, Eo. – Eoarchaean.

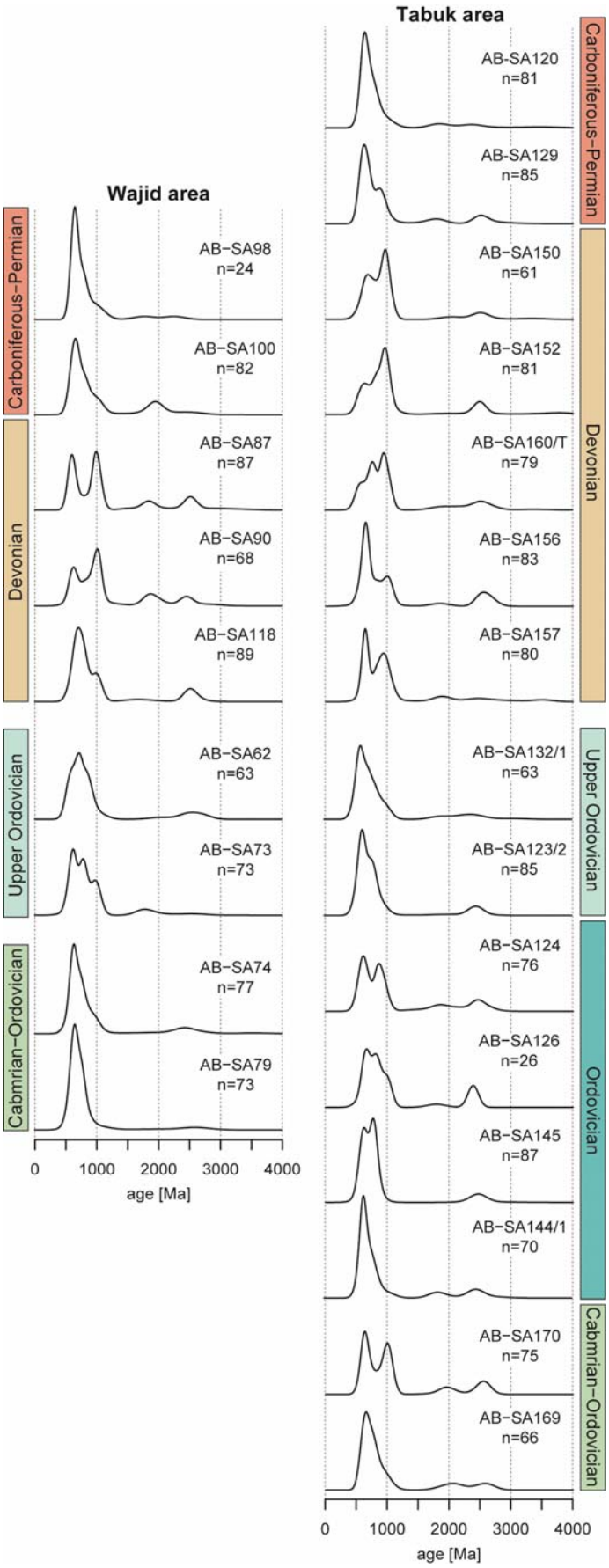

Fig. 6. (Colour online) Kernel density estimate (KDE) plots of the zircon age spectra in samples from the Wajid area (left) and Tabuk area (right) of Saudi Arabia. Samples are arranged from bottom to top according to their stratigraphic age. Only grains with 90 to 110% concordance are shown. n – number of zircon ages.

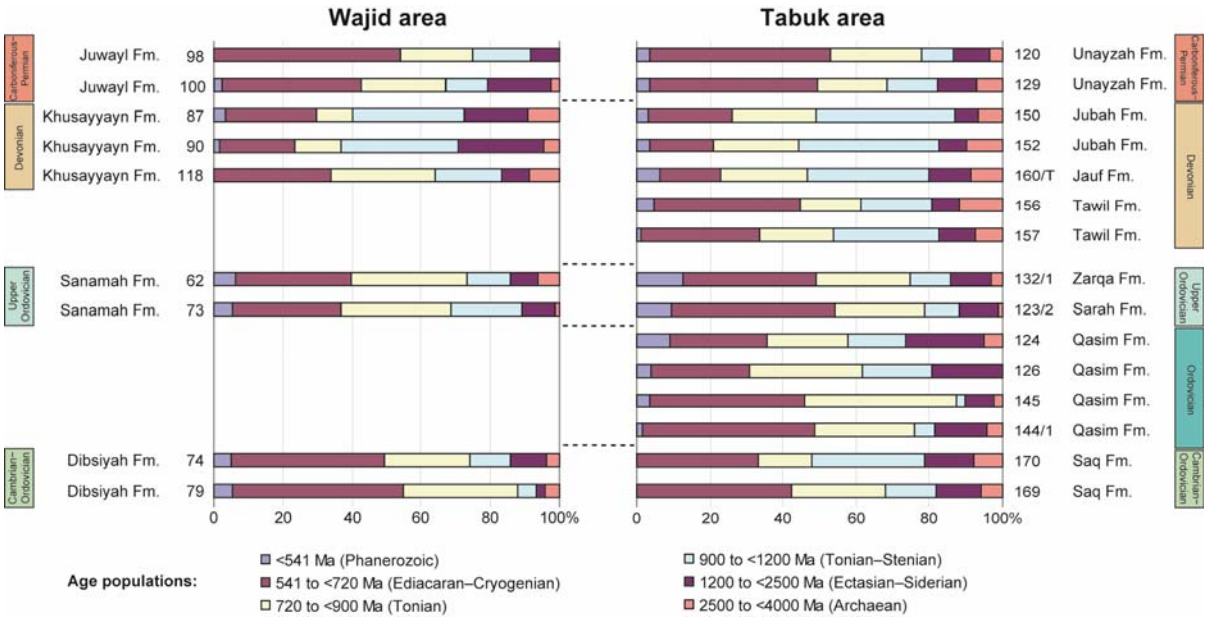

Fig. 7. (Colour online) Bar chart showing the relative abundances of the defined age groups in the analysed samples from the Wajid and Tabuk areas of Saudi Arabia. Samples are arranged from bottom to top according to their stratigraphic age.

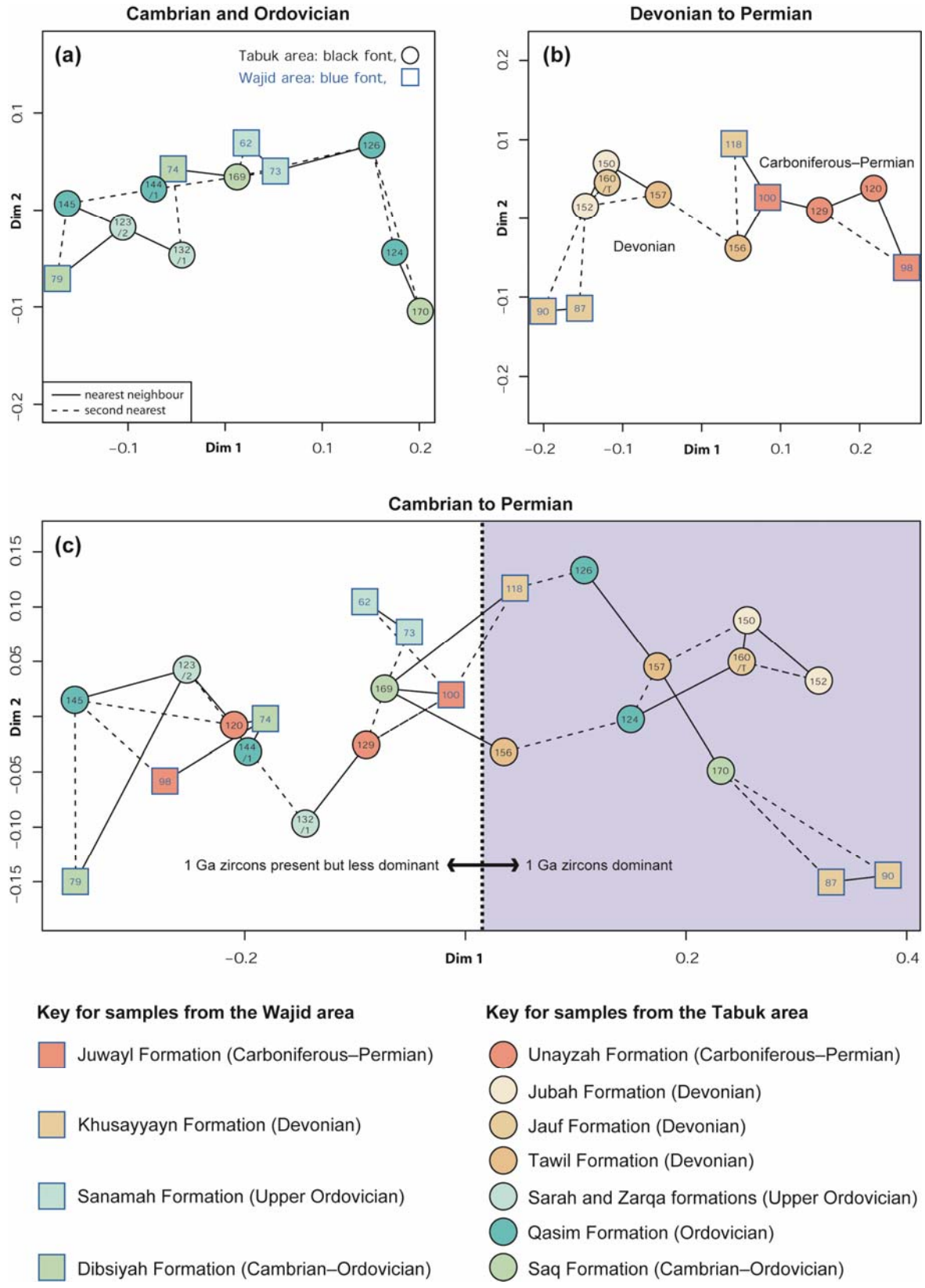

Fig. 8. (Colour online) Non-metric multidimensional scaling maps for the detrital zircon age spectra of Palaeozoic sandstone analysed in this study. Only ages >500 Ma are used here due to the low reliability of younger ages following Lewin *et al.* (2020a). The colours in the circles correspond to the colours used for the stratigraphy shown in Figure 3a.

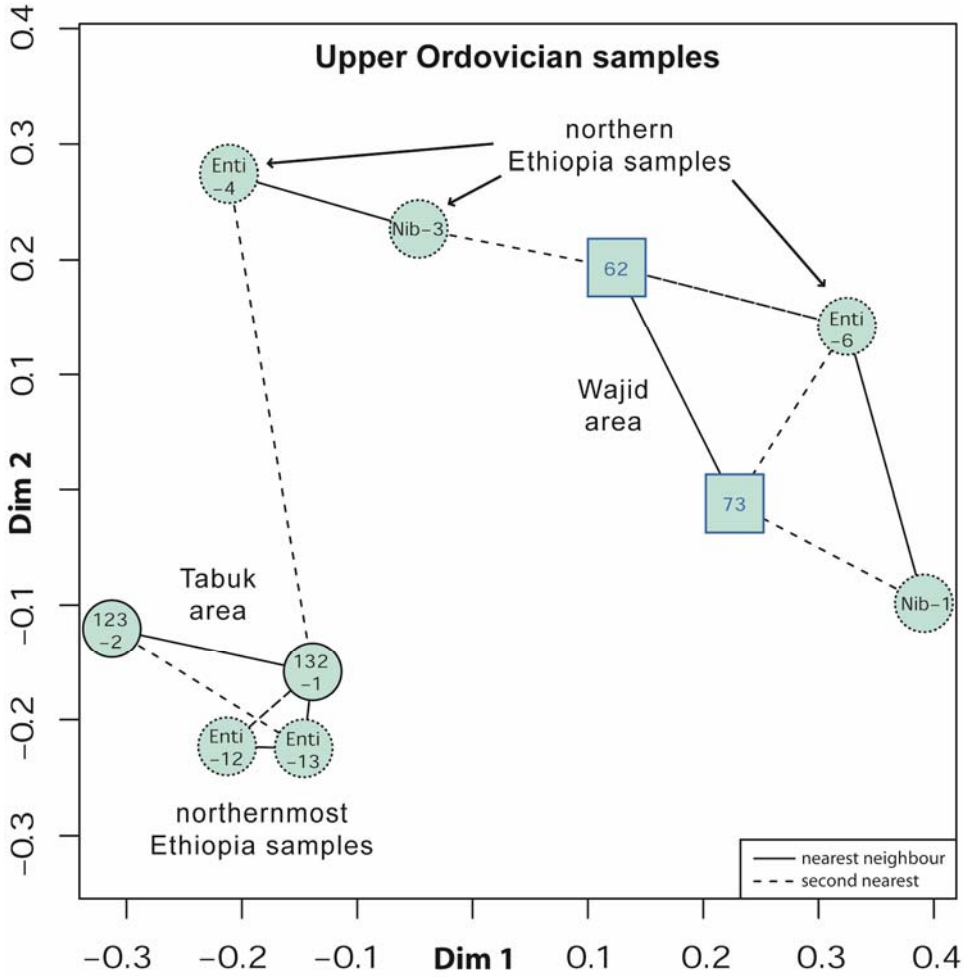

Fig. 9. Non-metric multidimensional scaling map comparing the detrital zircon age spectra of Upper Ordovician sandstones analysed in this study with published data from Upper Ordovician–Silurian sandstones of Ethiopia (data taken from Lewin *et al.* 2020a). Only ages >500 Ma are used here due to the low reliability of younger ages.

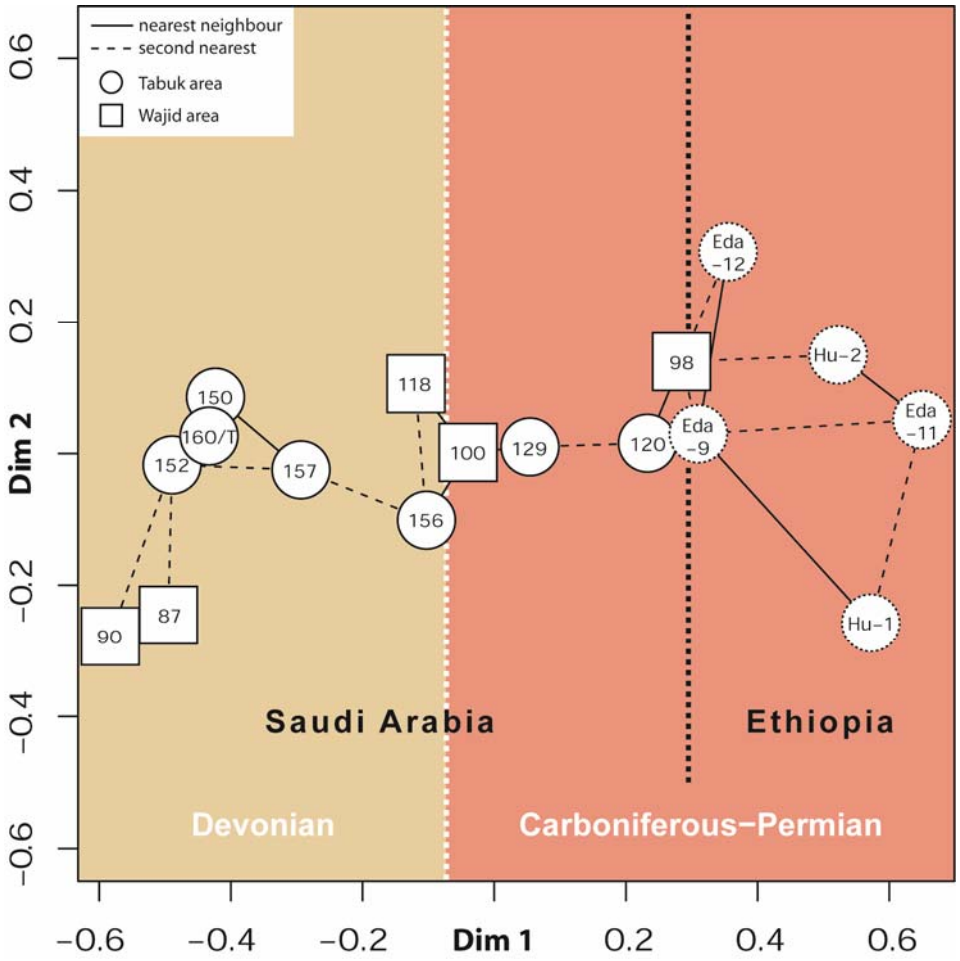

Fig. 10. (Colour online) Non-metric multidimensional scaling map comparing the detrital zircon age spectra of Devonian and Carboniferous–Permian sandstones analysed in this study with published data from Carboniferous–Permian sandstones of Ethiopia (data taken from Lewin *et al.* 2020a). Only ages >500 Ma are used here due to the low reliability of younger ages.

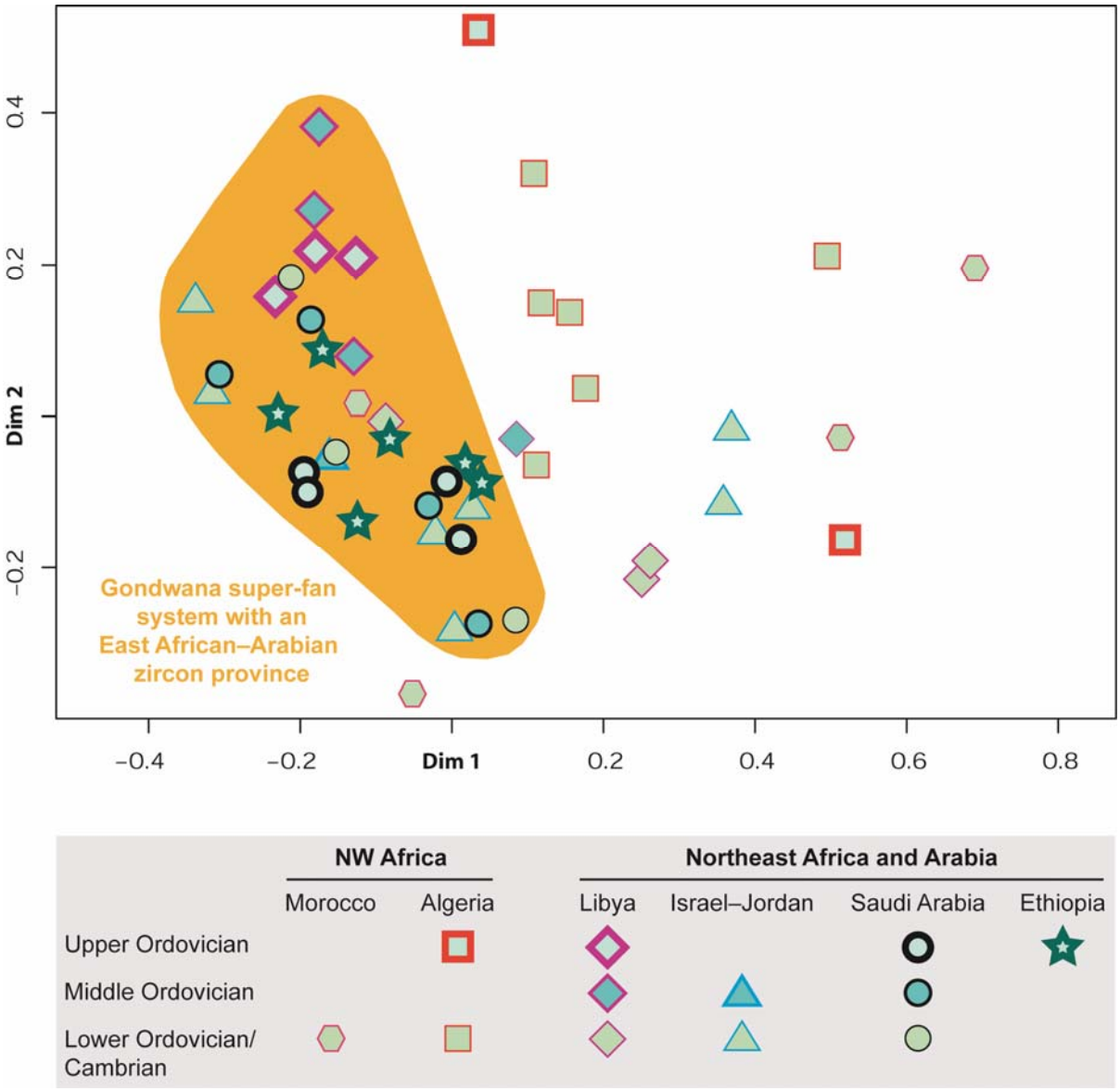

Fig. 11. (Colour online) Non-metric multidimensional scaling map comparing the detrital zircon age spectra of Cambrian–Ordovician sandstones analysed in this study with published data from Cambrian–Ordovician sandstones. Only ages >500 Ma are used here due to the low reliability of younger ages. Published data: (1) Meinhold *et al.* (2011); (2) Morton *et al.* (2012); (3) Linnemann *et al.* (2011); (4) Kolodner *et al.* (2006); (5) Altumi *et al.* (2013); (6) Avigad *et al.* (2012); (7) Lewin *et al.* (2020a). Note that the published data are those compiled by Meinhold *et al.* (2013) augmented by those from Altumi *et al.* (2013) and Lewin *et al.* (2020a). The orange field outlines the Gondwana super-fan sediments of northeast Africa and Arabia, as defined by Meinhold *et al.* (2013), which are characterized by detrital zircons with 'Pan-African' U–Pb ages accompanied by zircon grains with Tonian–Stenian (~1 Ga) and minor older ages. Sediments with such ages correspond to the East African–Arabian zircon province of Stephan *et al.* (2019a).

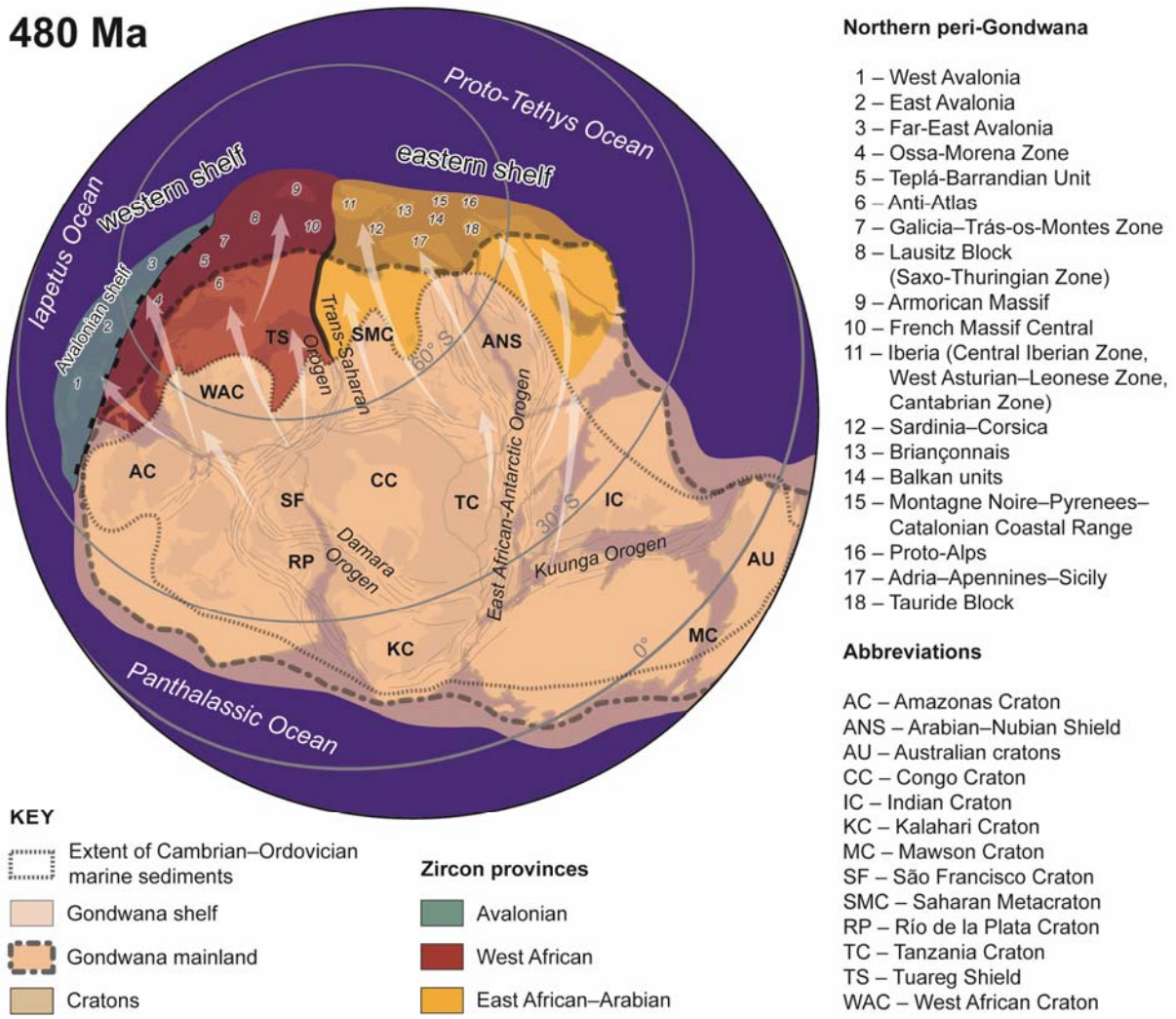

Fig. 12. (Colour online) Palaeogeographic reconstruction of Gondwana (480 Ma) modified after Stephan *et al.* (2019b) showing the main zircon provinces recognized in Cambrian–Ordovician siliciclastic sediments of northern Gondwana and its periphery. The East African–Arabian zircon province defined by Stephan *et al.* (2019a) corresponds to the zircon province of the Gondwana super-fan system of Meinhold *et al.* (2013). According to the detrital zircon U–Pb ages from Palaeozoic sandstones of Saudi Arabia (this study), the East African–Arabian zircon province can be extended to the central and southern Arabian Peninsula. White arrows show main sediment transport direction.

Table 1. Sample information. The samples are given for each study area in stratigraphic order from old (bottom) to young (top). Locations are given in geographical coordinates (WGS84). Detailed information on the petrography, whole-rock geochemistry and heavy mineral data of each sample is given in Bassis *et al.* (2016a,b). Last two columns: summary of detrital zircon ages of samples analysed in this study. Complete data sets used here are reported in Table S2 in the Supplementary Material.

Sample	Latitude/Longitude	Location	Age	Stratigraphy	Rock type	Number of ages determined	Number of ages used
Tabuk area							
AB-SA120	N 26°07′30.1″/E 043°59′11.7″	Buraida-Unayzah road	Carboniferous–Permian	Unayzah Formation	subarkose	85	81
AB-SA129	N 26°55′35.9″/E 043°34′39.8″	NW of Qusaiba	Carboniferous–Permian	Unayzah Formation	quartz arenite	90	85
AB-SA150	N 29°58′14.2″/E 040°10′19.4″	W of Sakaka	Devonian	Jubah Formation	subarkose	64	61
AB-SA152	N 29°58′17.7″/E 040°10′21.0″	W of Sakaka	Devonian	Jubah Formation	subarkose	85	81
AB-SA160/T	N 30°04′46.0″/E 039°55′52.0″	Wadi Murayr	Devonian	Jauf Formation	arkose	90	79
AB-SA156	N 29°49′30.5″/E 039°32′16.4″	W of Dawmut al Jandal	Devonian	Tawil Formation	quartz arenite	85	83
AB-SA157	N 29°49′29.3″/E 039°32′17.0″	W of Dawmut al Jandal	Devonian	Tawil Formation	subarkose	83	80
AB-SA132/1	N 26°51′28.6″/E 043°21′22.2″	NW of Al Qara	Upper Ordovician	Zarqa Formation	subarkose	77	63
AB-SA123/2	N 26°23′02.4″/E 043°45′41.8″	W of Al Qara	Upper Ordovician	Sarah Formation	quartz arenite	88	85
AB-SA124	N 26°23′25.1″/E 043°46′22.3″	W of Al Qara	Ordovician	Qasim Formation	quartz arenite	85	76
AB-SA126	N 26°34′10.4″/E 043°22′02.7″	Sarah ridge	Ordovician	Qasim Formation	subarkose	39	26
AB-SA145	N 27°43′14.2″/E 041°45′01.3″	N of Hail	Ordovician	Qasim Formation	quartz arenite	90	87
AB-SA144/1	N 27°40′09.0″/E 041°45′55.5″	Hail	Ordovician	Qasim Formation	quartz arenite	85	70
AB-SA170	N 26°48′41.1″/E 039°29′04.2″	along Highway 70	Cambrian–Ordovician	Saq Formation	quartz arenite	81	75
AB-SA169	N 26°27′54.7″/E 039°14′46.3″	along Highway 15	Cambrian–Ordovician	Saq Formation	quartz arenite	84	66
Wajid area							
AB-SA98	N 19°57′37.4″/E 044°44′59.0″	Jabal Seab	Carboniferous–Permian	Juwayl Formation	arkose	24	24
AB-SA100	N 19°57′37.1″/E 044°44′59.9″	Jabal Seab	Carboniferous–Permian	Juwayl Formation	quartz arenite	90	82
AB-SA87	N 20°04′50.6″/E 044°39′48.0″	Jabal Khusayyayn	Devonian	Khusayyayn Formation	subarkose	90	87
AB-SA90	N 20°04′53.9″/E 044°39′49.7″	Jabal Khusayyayn	Devonian	Khusayyayn Formation	subarkose	80	68
AB-SA118	N 18°10′21.8″/E 044°19′10.3″	Nawan	Devonian	Khusayyayn Formation	quartz arenite	90	89
AB-SA62	N 20°14′57.6″/E 044°17′13.8″	Jabal Atheer	Upper Ordovician	Sanamah Formation	sublitharenite	81	63
AB-SA73	N 20°09′17.0″/E 044°09′53.9″	Jabal Nafla	Upper Ordovician	Sanamah Formation	quartz arenite	83	73
AB-SA74	N 20°09′15.5″/E 044°09′53.3″	Jabal Nafla	Cambrian–Ordovician	Dibsiyah Formation	quartz arenite	83	77
AB-SA79	N 20°09′16.7″/E 044°09′34.4″	Jabal Nafla	Cambrian–Ordovician	Dibsiyah Formation	quartz arenite	83	73